THE EQUATION OF STATE OF LOW AND INTERMEDIATE DENSITY NUCLEAR MATTER WITH LIGHT AND MEDIUM CLUSTERS UP TO A = 50

معادلة الحالة للمادة النووية قليلة الكثافة ومتوسطتها والمحتوية على تجمعات أنوية خفيفة ومتوسطة حتى خمسين نيوكليوناً

By

RULA IMAD AL-DIN SAID BAKEER

Thesis committee:

Prof. Henry Jaqaman (Principal advisor)

Dr. Wafaa Khater (Member)

Dr. Hazem Abu Sara (Member)

This Thesis was submitted in partial fulfillment of the requirements for the Master's Degree in Physics from the Faculty of Graduate Studies at Birzeit University, Palestine.

February 1, 2018

THE EQUATION OF STATE OF LOW AND INTERMEDIATE DENSITY NUCLEAR MATTER WITH LIGHT AND MEDIUM CLUSTERS UP TO A = 50

By

RULA IMAD AL-DIN SAID BAKEER

Accepted by the Faculty of Graduate Studies, Birzeit University, in partial fulfilment of the requirements of the Master's Degree in Physics.

Thesis committee:

_____

Henry Jaqaman Ph.D. (Principal advisor)

_____

Wafaa Khater Ph.D. (Member)

_____

Hazem Abu Sara Ph.D. (Member)

February 1, 2018

DEDICATION

To the one who contributed for me to find the strength in life through her hope, my Mother! You are the breath of life.

To my Father who fill my days with joy and love. You give me the power to believe in my passion and pursue my dreams.

To my siblings. You are the corner stones of my life.

To Scientists for Palestine who supported me and lighted my life through their love and knowledge.

To my friends who never stopped giving love and happiness. You are my lucky charms.

God bless you all.

ACKNOWLEDGMENT

I extend sincere thanks and appreciation to Prof. Henry Jaqaman, who continuously conveyed to me a spirit of excitement regarding research and teaching. Without his continuous support and assistance, this thesis would not have been possible. I would like also to thank the members of my advisory committee, Dr. Hazem Abu Sara and Dr. Wafaa Khater, for their valuable comments and notes. My appreciations also go to all the faculty members at the Department of Physics; especially Prof. Edward Sader, who taught me how to find sight through physics. My thanks and heartfelt appreciations also go to my family and friends for their unquestionable and unconditional love.

TABLE OF CONTENTS

ABSTRACT

Nuclear matter at low and intermediate density and moderate temperature minimizes its energy by forming nuclear clusters. Most previous theoretical investigations ignored the formation of the heavy clusters and focused on light clusters with mass number up to A = 4. In this work, clusters with mass number up to A = 50 are included in nuclear matter and treated by the Nuclear Statistical Equilibrium model (NSE) which states that clusters are in chemical equilibrium with the free nucleons in the surrounding vapour. The Nuclear Statistical Equilibrium (NSE) model was modified by using density-dependent binding energies of clusters where the clusters' binding energies decrease as the surrounding medium density increases. In fact, clusters undergo the Mott transition and get dissolved as the density of nuclear matter increases due to the medium effects. The Pauli Blocking is found to be the prominent factor that affects clusters' binding energies. It was found that heavier clusters play a significant role in low and intermediate density symmetric nuclear matter composition and should be included in the equation of state (EoS) to make the study more realistic. Finally, these clusters reduce the critical temperature by several MeVs.

ملخص

تعمل المادة النووية ذات الكثافة المنخفضة ودرجات الحرارة المتوسطة على تقليل طاقتها بتكوين الانوية. اهتمت معظم الدراسات السابقة بدراسة المادة النووية قليلة الكثافة المحتوية على الأنوية ذات العدد الكتلي الذي لا يتجاوز الأربعة. أما في هذه الدراسة, فقمنا بالأخذ بالحسبان تكون الأنوية الأثقل التي تحتوي على خمسين نيوكليوناً على الأكثر وعالجناها باستخدام نموذج التوازن الإحصائي النووي الذي يفترض وجود اتزان كيميائي بين الأنوية والنيوكليونات الحرة في الوسط المحيط. تختلف خصائص هذه الأنوية عن الأنوية العادية المعزولة بسبب تأثيرات الوسط المحيط بها حيث تقل طاقة ربطها كلما ازدادت كثافة المحيط إلى أن تذوب في الوسط المحيط عندما تؤول طاقة ربطها إلى الصفر. يعد مبدأ باولي من أكثر العوامل تأثيراً على طاقة الربط للأنوية. لذلك قمنا بإدخال تعديل على نموذج التوازن الإحصائي النووي حيث استخدمنا طاقة الربط للأنوية المعتمدة على كثافة الوسط المحيط. لقد وُجد أن الأنوية الثقيلة تلعب دوراً مهماً في تركيب المادة النووية خصوصاً عند درجات الحرارة المنخفضة بحيث أنها تتواجد بنسب لا يمكن إهمالها ولذلك فمن الضروري إدراجها في معادلة الحالة للمادة النووية. في النهاية، وجود هذه الأنوية في دراسة المادة النووية قليلة الكثافة يُقلل درجة الحرارة الحرجة للمادة النووية مقارنة بمثيلتها التي يتم احتسابها بافتراض أن المادة النووية تتكون فقط من نيوكليونات منفصلة.

LIST OF FIGURES

LIST OF TABLES

CHAPTER 1

INTRODUCTION

The composition and the equation of state (EoS) of nuclear matter has been an important subject of numerous investigations in nuclear physics. In the past, scientists used to think that nuclear matter consists of only free protons and neutrons regardless of its density. However, at sub-saturation densities, correlations (clusters) are formed and nuclear matter becomes inhomogeneous [1-9]. In particular, this is important for nuclear matter at sub-saturation density which exists in the crust of neutron stars and in the envelope of core-collapse supernovae [10-12] and which gains the attention of cosmologists and astronomers.

These bound states (clusters) change the composition of nuclear matter and affect its thermodynamical behaviour. The occurrence of clusters also minimizes nuclear matter energy [7]. In general, the formation of clusters varies with nuclear matter density and temperature whereas clusters dissolve with increasing density due to the decrease in their binding energies.

Pauli Blocking is one of the main medium effects on the cluster properties as it causes its binding energy to decrease as the medium density increases [13]. At a certain density called the Mott density, the binding energy vanishes and the cluster dissolves and its nucleons become free. Hence the cluster's binding energy has to

take density-dependent form to include the medium effects. That is why the clustering is limited to low and intermediate densities.

Röpke et al studied a homogeneous system of free nucleons and composite particles which are states of bound nucleons and discussed its thermodynamic properties in 1982 [1]. They studied especially the abundance of deuterons immersed in a medium of free nucleons by using the Bethe-Goldstone equation for thermodynamic Green functions. After one year, Röpke et al extended their work by including helions, tritons and alpha particles as well as deuterons and included medium effects in the equation of state [2]. Helions are the nuclei of ^{3}He and consist of two protons and one neutron while the tritons are the nuclei of ^{3}H and consist of two neutrons and one proton. However, they ignored the difference in binding energy between helion and triton. They concluded that the cluster formation leads to a reduction in the critical temperature of nuclear matter by 2.5 MeV.

The stability of hot nuclei immersed in a vapour of free nucleons was studied by Levit and Bonche in 1985 [14] by using an equation of state of nuclear matter derived on the basis of the Hartree-Fock approximation with an effective nucleon-nucleon interaction of the Skyrme type. They emphasized that such nuclei cannot exist above a certain temperature which they called the limiting temperature. The limiting temperature depends strongly on the properties of the nuclear matter contained in its equation of state, and also on the surface tension of the nuclei.

Levit and Bonche's equation of state was generalized by Jaqaman to describe asymmetric nuclear matter [3]. In another study [15], Jaqaman improved the equation of state in [3] by taking into account the density-dependent nucleonic effective mass and the vapour's electric charge and showed that the vapour electric charge raises the limiting temperatures.

Light clusters with mass number up to A = 4 were included by Beyer et al [4] in a study which depends on the statistical model and the Hartee-Fock (HF) approximation for the quasi-particle energy. They concluded that the composition of nuclear matter with light clusters at finite temperatures varies with nuclear matter temperature, density and CM momentum of clusters.

Horowitz and Schwenck constructed a low density nuclear matter equation of state in 2006 by including protons, neutrons and alpha particles [6]. Their work was based on the nuclear statistical equilibrium model and the virial expansion. They concluded that alpha particles form as the nuclear matter density increases, which leads to a significant reduction of the pressure of low density nuclear matter.

In 2008, the appearance of light clusters with mass number up to A = 4 in core-collapse supernova was studied by Sumiyoshi and Röpke by using a quantum statistical approach. They found that deuterons, tritons, helions and alphas appear strongly in a wide region from the surface of the proto-neutron star which is a tiny survivor star after supernova explosions [16].

The basic properties of light clusters in hot and dense nuclear matter were studied by Röpke in 2009 [13] by using Green's function at different limits. At first, at low density limit where nuclear statistical (NSE) and virial models are valid. Secondly, at high density limit where relativistic mean field model (RMF) is valid. He included clusters with mass number up to A = 4 and ignored high density region as temperature goes down because he predicted that heavier clusters with mass number ($A > 4$) will appear there and become more important. He noticed that results deviate from nuclear statistical equilibrium (NSE) model at densities that exceed 10^{-4} nucleon/fm^3 due to the medium modification effects.

Heckel et al included clusters with mass number up to $A \leq 13$ in the equation of state (EoS) of low density supernova matter and determined its composition [17]. They found that these clusters lower the critical temperature.

Typel et al [7] investigated the composition of nuclear matter at finite density and temperature ($T \leq 20$) including light clusters with mass number up to A = 4 by using a microscopic quantum statistical (QS) approach and a generalized relativistic mean field (RMF) model. Both approaches give the same results as the nuclear statistical equilibrium (NSE) model in the low density limit as shown in the study. They modified the properties of the clusters by including the medium effects on their binding energies. This eventually leads to the dissolution of the clusters due to the reduction in their binding energies as the medium density increases. Cluster dissolution occurs when the binding energy goes to zero due to the medium effect of

Pauli Blocking. This dissolution is known as the Mott transition. They found that the composition of nuclear matter with clusters varies as its density and temperature changes. They found that alpha particles are dominant at low temperatures ($T \leq 2MeV$) and low densities (less than 10^{-2} nucleon/fm^3) but at higher temperatures the deuterons are dominant at these densities. They also discussed the effect of clusters formation on the liquid-gas phase transition and other thermodynamical quantities. However, they mentioned that the formation of clusters reduces the entropy per nucleon of symmetric nuclear matter as compared to pure neutron-proton matter without clusters. This point is explained in Appendix A to clarify that it does not conflict with the Second Law of Thermodynamics.

The limiting temperature for hot nuclei which are in thermal, chemical and mechanical equilibrium with the surrounding vapour including clusters was studied by Talahmeh and Jaqaman [18]. They included clusters with mass number up to A = 4 in the vapour and found that the presence of these clusters reduced the limiting temperature by several MeVs. However, W. Awad study [19] included clusters with mass number up to A = 25 in low density symmetric nuclear matter and emphasized that these clusters must be considered in low density symmetric nuclear matter equation of state as their presence reduces the critical temperature of the system.

There has also been definite experimental evidence for an abundance of light clusters in nuclear matter at low density and moderate temperatures [20-22]. In general they this was observed in the abundant emission of light particles in low energy heavy-ion

collisions. For example, [22] presented a first experimental determination of in medium cluster binding energies and Mott points for light clusters (d, t, h and α) in low density nuclear matter produced in collisions of ^{40}Ar and ^{64}Zn projectiles with ^{112}Sn and ^{124}Sn target nuclei. Where the kinetic energy per nucleon of projectile nuclei is 47 MeV. Their results were in good agreement with those predicted by recent theoretical predictions based upon the implementation of Pauli blocking effects in a quantum statistical approach in [7].

In the present thesis, we consider the formation of light and medium clusters with mass number up to A = 50 in the nuclear vapour by using a modified form of the nuclear statistical equilibrium model (NSE) that includes the medium modification of the clusters properties. We also examine how the value of the critical temperature ($T_{critical}$) is affected by the inclusion of clusters with mass number up to A = 50 in the vapour state of nuclear matter at low and intermediate densities up to $\rho = 0.1$ nucleon/fm^3.

In Chapter 2, we describe the equation of state of ideal quantum gases. In Chapter 3, we construct the equation of state of nuclear matter consisting of nucleons interacting via the Skyrme effective interaction and study its behaviour at different temperatures to determine its critical point. In Chapter 4, we review various theoretical investigations of clustered nuclear matter and focus on the Nuclear Statistical Equilibrium model. In Chapter 5, we determine the composition of clustered symmetric nuclear matter by including clusters with mass number up to A = 50 at

different temperatures. Finally, we discuss our results and present our conclusions in Chapter 6.

CHAPTER 2

EQUATION OF STATE OF IDEAL QUANTUM GASES

The ideal quantum gas can be defined as a system of indistinguishable non-interacting particles that obey Fermi-Dirac or Bose-Einstein statistics. The equation of state is a thermodynamic mathematical relation which relates the system density to the other main system variables, like its pressure, volume and temperature. Each system has its own fundamental characteristic equation of state [23].

In this chapter, we will discuss an infinite system of non-interacting fermions and bosons respectively, and mention the equation of state for them to use it later in constructing the clustered nuclear matter equation of state.

2.1 IDEAL FERMI GAS EQUATION OF STATE

The ideal Fermi gas is a physical system consisting of a large number of non-interacting identical fermions. It is the quantum mechanical version of an ideal gas. Fermions are particles whose spin quantum number is half an integer. These particles follow Fermi-Dirac statistics where it is prohibited that two identical fermions with same quantum numbers occupy the same quantum state, this is known as the Pauli Exclusion Principle [24].

Protons and neutrons are fermions, they differ in their electromagnetic properties because of the positive charge that the proton has. They both are treated in the same way if the Coulomb force interactions between protons are switched off. So we can say that the proton and neutron are two states of the same particle called the nucleon with mass nearly 940 MeV/c^2. A system of nucleons at low densities can be classified as an ideal Fermi gas.

The Fermi-Dirac distribution function $\frac{1}{e^{\beta(\varepsilon_i - \mu)}+1}$ for a system consists of N identical fermions with single fermion energies of ε_i satisfies the relation [23]:

$$\frac{N}{g} = \sum_i n_i = \sum_i \frac{1}{e^{\beta(\varepsilon_i - \mu)} + 1} \tag{2.1}$$

where g is the spin-isospin degeneracy factor that arises from the internal structure of particles such as spin s and isospin I ($g = (2s + 1)(2I + 1)$), n_i is the probability that the ith energy level is occupied by a single fermion at absolute temperature T, μ is the fermionic chemical potential which we will discuss later in this chapter and $\beta = 1/k_B T$ where k_B is the Boltzmann constant.

We can use energy units instead of Kelvins for the temperature by multiplying the absolute temperature by Boltzmann's constant:

$$k_B = 8.617 \times 10^{-11}\ \text{MeV/Kelvin}$$

In these units a temperature of 1 MeV is equivalent to T = (1.16×10^{10}) Kelvin in SI units. From now on, I will use T in MeV instead of $k_B T$, and it will have energy units.

The equation of state for an ideal gas of non-interacting identical fermions can be expressed as an equation for the chemical potential $\mu(T, \rho)$ or the pressure $P(T, \rho)$ [3, 18]:

$$\mu(T, \rho) = T \left[\ln\left(\frac{\lambda_T^3 \rho}{g}\right) + \sum_{n=1}^{\infty} b_n \left(\frac{\lambda_T^3 \rho}{g}\right)^n \right] \tag{2.2}$$

$$P(T, \rho) = T \rho \left[1 + \sum_{n=1}^{\infty} \frac{n}{n+1} b_n \left(\frac{\lambda_T^3 \rho}{g}\right)^n \right] \tag{2.3}$$

where ρ is the number density of the fermions, $\lambda_T = \left(\frac{2\pi\hbar^2}{m\,T}\right)^{\frac{1}{2}}$ is the thermal wavelength of a fermion which is roughly the mean de Broglie wavelength of the gas particles in an ideal gas at the specified temperature T, g is the spin-isospin degeneracy factor (g = 4 for a gas of nucleons). The coefficients b_n up to n = 6 were evaluated in [18, 25] and are listed in Table 2.1. These coefficients reflect the higher order degeneracy corrections that significantly modify the chemical potential and pressure of an ideal Fermi gas as compared to those for an ideal classical gas. These coefficients have alternating signs and with increasing the order n they rapidly decrease. The contribution of higher order b_n coefficients in the equation of state decreases as temperature increases and can be ignored as will be seen later in this

chapter. Especially at T ≥ 4MeV, the contribution is negligible for densities up to 0.1 nucleon/fm^3.

Table 2.1: Numerical values of the b coefficients evaluated for the ideal Fermi gas.

	b_n
$n = 1$	0.3535533905933
$n = 2$	$-$ 0.0049500897299
$n = 3$	$1.483857713 \times 10^{-4}$
$n = 4$	$-4.4256301 \times 10^{-6}$
$n = 5$	1.006362×10^{-7}
$n = 6$	-4.272×10^{-10}

In our work, we deal with an infinite ideal Fermi gas of non-interacting fermions. The single particle energies in Eq. 2.1 are given in this case by

$$\varepsilon_k = \frac{\hbar^2 k^2}{2\,m}$$

where $k = 2\pi/\lambda$ is fermion wave number, and m is the fermion mass.

To investigate the convergence of Eqs. 2.2 and 2.3, the pressure of an infinite system of ideal nucleons is evaluated at different temperatures and up to different orders of n.

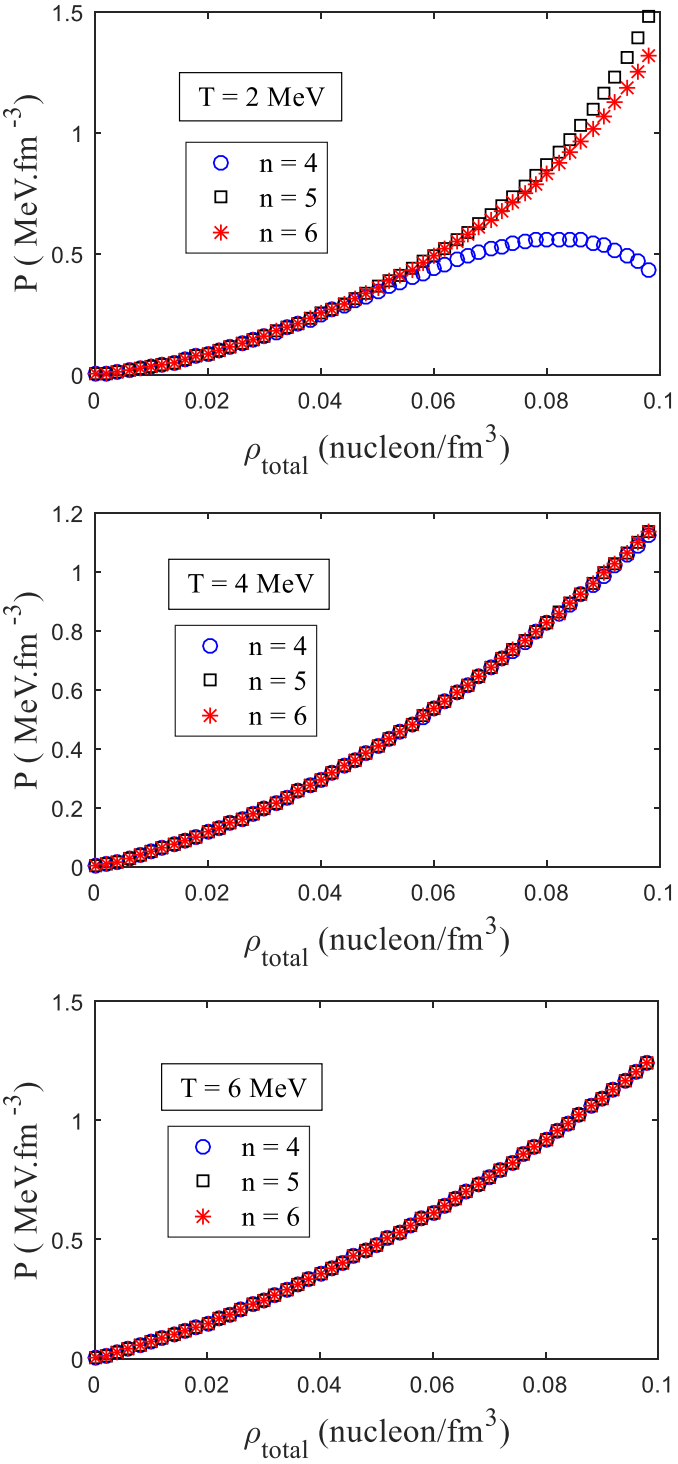

Fig. 2.1: The pressure of an ideal nucleons gas at different temperatures showing the effect of including terms up to order n.

It is clear from Fig. 2.1 that the convergence of the series depends on the temperature. At T = 2 MeV the pressure series converges at low densities up to about 0.06 nucleon/fm^3. The n = 6 term modifies the pressure summation at 0.1 nucleon/fm^3 by only about 12%. However, at the higher temperatures the pressure series still converge up to 0.1 nucleon/fm^3 which means that the contribution of higher orders of n is negligible for T $\geq$ 4 MeV. For example at T = 4 MeV the n = 6 term modifies the pressure at the density of 0.1 nucleon/fm^3 by only 0.06%. Hence in our work we will be satisfied with the first six terms in Eqs. 2.2 and 2.3 because we will not deal with system densities that exceed 0.1 nucleon/fm^3.

2.2 IDEAL BOSE GAS EQUATION OF STATE

The ideal Bose gas is a physical system consisting of a large number of non-interacting identical bosons, it is also the quantum mechanical version of an ideal gas. Bosons are particles whose spin quantum number is an integer, and they follow Bose-Einstein statistics.

At low temperatures close to absolute zero, all ideal gas bosons accommodate in the ground state at the same time, this phenomenon is called Bose-Einstein Condensation. However, that is not allowed for an ideal Fermi gas as mentioned before because of the Pauli Exclusion Principle.

The Bose-Einstein distribution function $\frac{1}{e^{\beta(\varepsilon_i - \mu)}-1}$ for a system consisting of N bosons with the single Bose particle energies ε_i satisfies the relation [23]:

$$\frac{N}{g} = \sum_i n_i = \sum_i \frac{1}{e^{\beta(\varepsilon_i - \mu)} - 1} \tag{2.4}$$

Where n_i is the probability that the ith energy level is occupied by a single boson at temperature T, and μ is the bosonic chemical potential.

The Ideal Bose gas chemical potential and pressure can be formulated as [18]:

$$\mu(T, \rho) = T \left[\ln\left(\frac{\lambda_T^3 \rho}{g}\right) + \sum_{n=1}^{\infty} d_n \left(\frac{\lambda_T^3 \rho}{g}\right)^n \right] \tag{2.5}$$

$$P(T, \rho) = T \rho \left[1 + \sum_{n=1}^{\infty} \frac{n}{n+1} d_n \left(\frac{\lambda_T^3 \rho}{g}\right)^n \right] \tag{2.6}$$

Where $d_n = (-1)^n b_n$ are the Bose gas coefficients and the b_n coefficients are given by table 2.1.

To investigate the convergence of Eqs. 2.5 and 2.6, the pressure of an ideal bosonic infinite system is plotted at different temperatures and orders of n as shown in Fig. 2.2. I choose a gas of non-interacting alpha particles which is classified as bosonic ideal gas since the alpha particle has spin zero. The alpha particle spin is zero, so the spin degeneracy factor for non-interacting alpha particles gas is equal to 1.

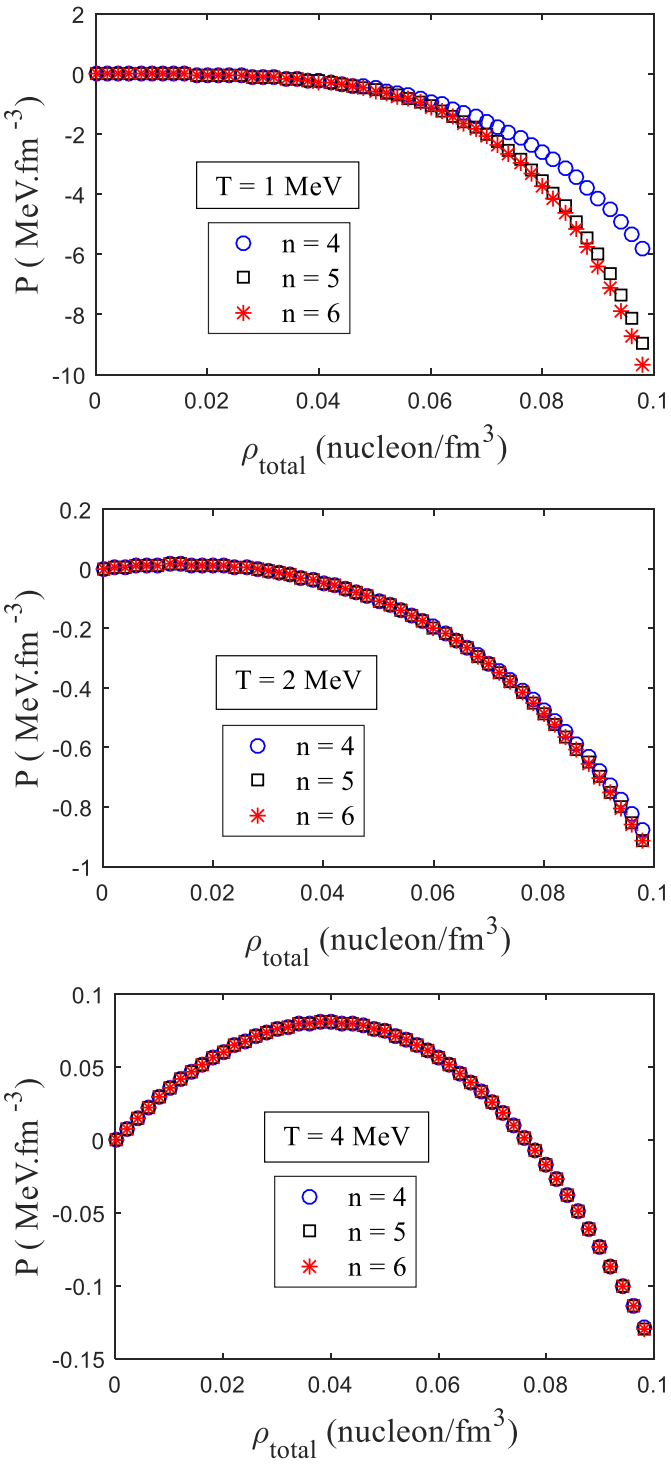

Fig. 2.2: The pressure of ideal alpha particles gas at different temperatures including terms up to order n.

The negative pressure at low temperatures reflects the Bose-Einstein Condensation phenomenon. By making comparison between Fig. 2.1 and Fig. 2.2, it is obvious that the pressure series for an ideal bosonic gas converges up to higher densities than the ideal fermionic gas. That is due to the higher mass of alpha particles compared with nucleons mass which affects the thermal wavelength and makes it smaller. For this bosonic ideal gas, the pressure series converges at low densities up to about 0.05 nucleon/fm^3 at T = 1 MeV as illustrated in the upper part of Fig. 2.2. However, the n = 6 term modifies the pressure summation at T = 1 MeV by 9% at 0.1 nucleon/fm^3 but at T = 2 MeV its effect does not exceed 0.3%. So the summation to the first six terms will be satisfactory since the convergence of the pressure series of bosonic ideal gas is assured at higher temperatures for densities up to 0.1 nucleon/fm^3.

CHAPTER 3

SKYRME EFFECTIVE INTERACTION AND NUCLEAR MATTER EQUATION OF STATE

Nucleons in nuclear matter interact with each other via the nuclear force. We will use a simple parameterization of the nuclear force called the Skyrme interaction [26].

3.1 SKYRME EFFECTIVE INTERACTION MODEL

The Skyrme interaction was proposed by Skyrme in 1962, and then used by Vautherin and Brink [27] to obtain the properties of finite nuclei as well as infinite nuclear matter. In this work we will use a zero-range Skyrme force in addition to switching off the Coulomb force between the protons,

$$v_{12} = -t_0\delta(\vec{r}_1 - \vec{r}_1) + \frac{t_3}{6}\rho^{\sigma}\left[\frac{\vec{r}_1 + \vec{r}_2}{2}\right]\delta(\vec{r}_1 - \vec{r}_2) \tag{3.1}$$

where v_{12} is the two-body Skyrme interaction between two nucleons, $\vec{r}_1$ and $\vec{r}_2$ are the position vectors of the two nucleons relative to a reference point, ρ is the nuclear matter density and σ is a parameter that controls nuclear matter incompressibility without changing its binding energy [25]. The incompressibility is a measure of the relative volume change of a fluid or solid as a response to a pressure change and is given by

$$K = -\frac{1}{V}\frac{\partial P}{\partial V}$$

where V and P are the nuclear matter volume and pressure respectively. The minus sign ensures that the incompressibility quantity is always positive.

The Skyrme interaction as illustrated in Eq. 3.1 has a density-dependent component, which implies that the interaction between two specified nucleons is affected by the existence of other nucleons in the nuclear matter (three-body forces).

The Skyrme interaction parameters t_0 and t_3 are related to the parameters a_0 and a_3 of the equation of state of interacting nuclear matter [see Eqs. 3.13 and 3.14 below] by the following relations [3]:

$$a_0 = \frac{3}{8} t_0 \tag{3.2}$$

$$a_3 = \frac{1}{16} t_3 \tag{3.3}$$

These parameters together with σ can be determined phenomenologically by fitting the ground state properties of nuclear matter [3]:

$$\sigma = \frac{(K - 9\,E_B - E_K)}{(9\,E_B + 3\,E_K)} \tag{3.4}$$

$$a_0 \rho_0 = \frac{\left[(1 + \sigma)\,E_B + \left(\sigma + \frac{1}{3}\right) E_K\right]}{\sigma} \tag{3.5}$$

$$a_0 \rho_0^{1+\sigma} = \frac{\left(E_B + \frac{E_K}{3}\right)}{\sigma} \tag{3.6}$$

where E_B is the nuclear matter binding energy per particle, whereas E_K is the nuclear matter kinetic energy per particle. ρ_0 is called the saturation density which is defined as the uniformly-distributed density inside a large-radius heavy nucleus [3, 14]:

$$\rho_0 = 0.17 \text{ nucleon/fm}^3$$

This value is not the same value of finite-nuclei average density which is defined as $\rho = \frac{A}{\frac{4}{3}\pi R^3}$ for mean nuclear radius $R = r_0 A^{1/3}$, where $r_0 = 1.2$ fm. As a result, the average density is found to be constant for any nucleus regardless of its mass number and can be approximated to 0.14 nucleon/fm^3. The difference between these two values is attributed to the absence of the surface region in infinite nuclear matter [24].

Infinite nuclear matter binding energy per particle can be determined from the Weizsaecker (semi-empirical) mass formula for the binding energy B(Z,N) of a nucleus consists of Z protons and N = A – Z neutrons [24],

$$B(\mathrm{Z},\mathrm{N}) = \alpha_1 A - \alpha_2 A^{2/3} - \alpha_3 \frac{\mathrm{Z}(\mathrm{Z}-1)}{A^{1/3}} - \alpha_4 \frac{(\mathrm{N}-\mathrm{Z})^2}{A} + \Delta \qquad (3.7)$$

$\alpha_1, \alpha_2, \alpha_3, \alpha_4$ and Δ are determined by fitting experimental binding energy data for some nuclei, this is why it is called semi-empirical formula. The common values are [24]:

$\alpha_1 = 16$ MeV is called the volume energy parameter.

$\alpha_2 = 17$ MeV is called the surface energy parameter.

$\alpha_3 =$ 0.6 MeV is called the coulomb energy parameter.

$\alpha_4 =$ 25 MeV is called the symmetry energy parameter.

Δ is the pairing energy parameter and it is given by:

$$\Delta = \begin{Bmatrix} \delta & even-even\ nuclei \\ 0 & odd-even\ nuclei \\ -\delta & odd-odd\ nuclei \end{Bmatrix} \text{ where } \delta = \frac{25}{A} \text{ MeV}$$

In many cases it is better to use the binding energy per nucleon:

$$\frac{B(\mathrm{Z},\mathrm{N})}{A} = \alpha_1 - \frac{\alpha_2}{A^{1/3}} - \alpha_3 \frac{\mathrm{Z}\,(\mathrm{Z}-1)}{A^{4/3}} - \alpha_4 \frac{(\mathrm{N}-\mathrm{Z})^2}{A^2} + \frac{\Delta}{A} \qquad (3.8)$$

For finite nuclei, the binding energy per nucleon is around 8 MeV for most heavy nuclei with mass number larger than twenty $(A > 20)$ as illustrated in Fig. 3.1.

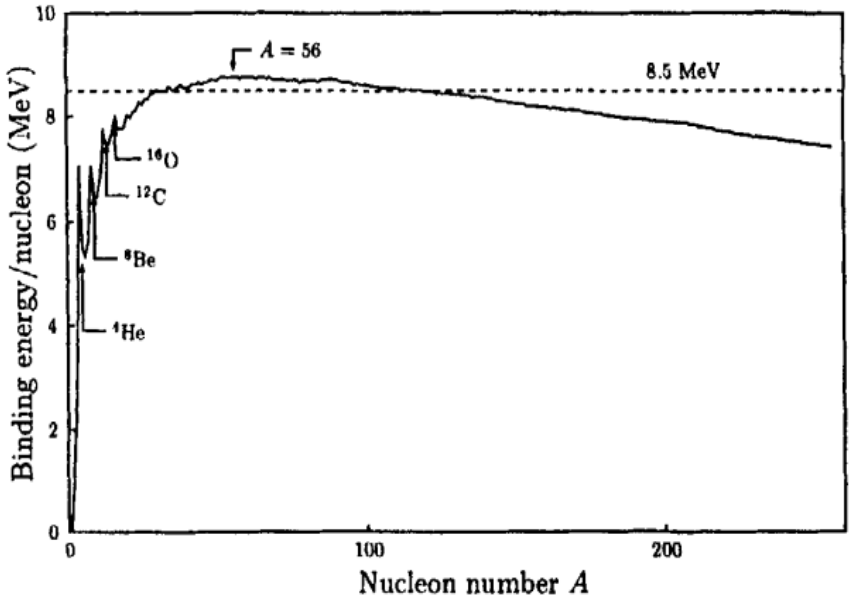

Fig. 3.1: The binding energy per nucleon for finite nuclei [24].

For infinite nuclear matter; which is described as an idealized system of an infinite number of nucleons interacting via the nuclear strong force with the Coulomb force switched off, the surface energy term vanishes since it is proportional to $A^{-1/3}$. The Coulomb term is also equal to zero due to switching off the Coulomb repulsion between protons. Moreover, we shall assume that the proton number is equal to the neutron number $(\mathrm{Z} = \mathrm{N})$. Such a system is called symmetric nuclear matter which leads to symmetry energy term cancellation. At last, we are dealing with an infinite number of nucleons so the pairing term goes to zero. Now the binding energy per nucleon for infinite nuclear matter is given by the following relation:

$$\frac{B(\mathrm{Z},\mathrm{N})}{A} = \alpha_1 \tag{3.9}$$

Hence, infinite symmetric nuclear matter binding energy per nucleon (E_B) is 16 MeV.

Infinite nuclear matter kinetic energy per particle can be determined by using Fermi gas model. Whereas the kinetic energy depends on Fermi momentum k_f and given by [23]:

$$E_K = \frac{3}{5}\frac{\left(\hbar k_f\right)^2}{2\, m_{nucleon}} = \frac{3}{5}\varepsilon_f \tag{3.10}$$

$$k_f = \left(\frac{3\,\pi^2}{2}\rho_0\right)^{1/3} \tag{3.11}$$

By substituting $\rho_0 = 0.17$ MeV in Eq. 3.11, the Fermi momentum is $k_f = 1.36$ fm^{-1}. Hence infinite nuclear matter kinetic energy per particle (E_K) is 24 MeV. However, the kinetic energy per particle for finite nuclei is 20 MeV by using the average density for finite nuclei $\rho = 0.14$ nucleon/fm^3 instead of the saturation density in Eq. 3.11 and the Fermi momentum is $k_f = 1.27$ fm^{-1} for finite nuclei.

The Skyrme interaction parameters are listed in table 3.1, these parameters will be used later in this chapter.

Table 3.1: Skyrme interaction parameters [3, 14].

	$a_0\rho_0(MeV)$	$a_3\rho_0^{1+\sigma}(MeV)$	K (MeV)
$\sigma = 1$	64	24	384
$\sigma = 0.25$	136	96	222

3.2 SYMMETRIC NUCLEAR MATTER EQUATION OF STATE INCLUDING SKYRME INTERACTION

The ideal Fermi gas equation of state was discussed in chapter 2 where the nucleon-nucleon interaction was ignored. If the nucleons interact via the Skyrme force only, we can extend the results of chapter 2 by including Skyrme force effects. The main effect will be on the single particle energies of the nucleons in symmetric nuclear matter with switching off the Coulomb force,

$$\varepsilon_k = \frac{\hbar^2 k^2}{2\,m} + \varepsilon_0 \tag{3.12}$$

where $\varepsilon_0 = -\frac{3}{4}t_0\,\rho + \frac{3}{24}t_3\left[1+\frac{\sigma}{2}\right]\rho^{1+\sigma}$ is the Skyrme single-particle energy term [27].

The pressure and chemical potential of symmetric nuclear matter with Skyrme interaction equations of state respectively as derived by Jaqaman [3, 15],

$$\tilde{\mu}(T,\rho) = -2\,a_0\,\rho + a_3(2+\sigma)\rho^{(1+\sigma)} + T\left[\ln\left(\frac{\lambda_T^3\,\rho}{g}\right) + \sum_{n=1}^{\infty} b_n\left(\frac{\lambda_T^3\,\rho}{g}\right)^n\right] \tag{3.13}$$

$$\tilde{P}(T,\rho) = -a_0\rho^2 + a_3(1+\sigma)\rho^{(2+\sigma)} + T\,\rho\left[1 + \sum_{n=1}^{\infty}\frac{n}{n+1}\,b_n\left(\frac{\lambda_T^3\,\rho}{g}\right)^n\right] \tag{3.14}$$

where $g = 4$ is the nucleon spin-isospin degeneracy factor.

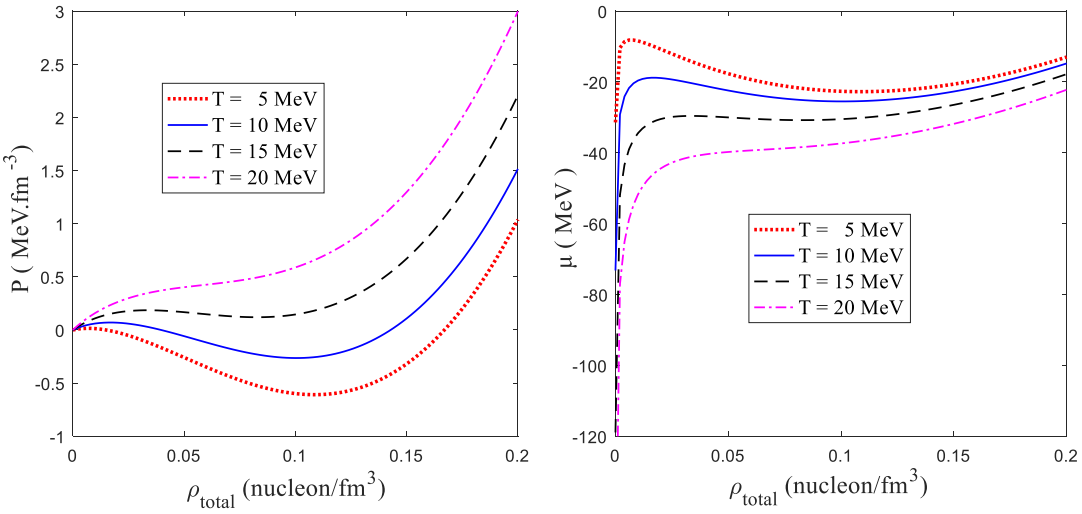

Fig. 3.2: The pressure and chemical potential isotherms for symmetric nuclear matter including Skyrme interaction at different temperatures with $\boldsymbol{\sigma = 0.25}$.

The Pressure and Chemical potential isotherms for symmetric nuclear matter with the Skyrme interaction are shown in Fig. 3.2. Both sets of isotherms increase with density until they reach to a maximum value before dropping to a minimum and rising again. Their behaviour is the same as that of the Van der Waals equation of state. Each isotherm consists of three regions; the first one is the low-density vapour region where the pressure increases with density. The second is the intermediate-density region where the isotherm has a negative slope and is thus mechanically unstable. The third is the high-density liquid region. As the temperature increases the maxima and minima become less prominent until they disappear as can be seen for the T = 20 MeV isotherms.

At a certain temperature which is called the critical temperature, the pressure or chemical potential isotherm has one inflection point; the maximum and minimum will merge. This inflection point is called the critical point and defined as [28]

$$\frac{\partial P}{\partial \rho} = \frac{\partial^2 P}{\partial^2 \rho} = 0 \left[or \ \frac{\partial \mu}{\partial \rho} = \frac{\partial^2 \mu}{\partial^2 \rho} = 0 \right] \tag{3.15}$$

Hence, above the critical temperature the pressure and chemical potential isotherms monotonically increase as density increases and only one fluid phase exists. So T = 20 MeV is located above the critical temperature due to isotherms continuously increasing with density. In particular the critical temperature must be located between 15 and 20 MeV.

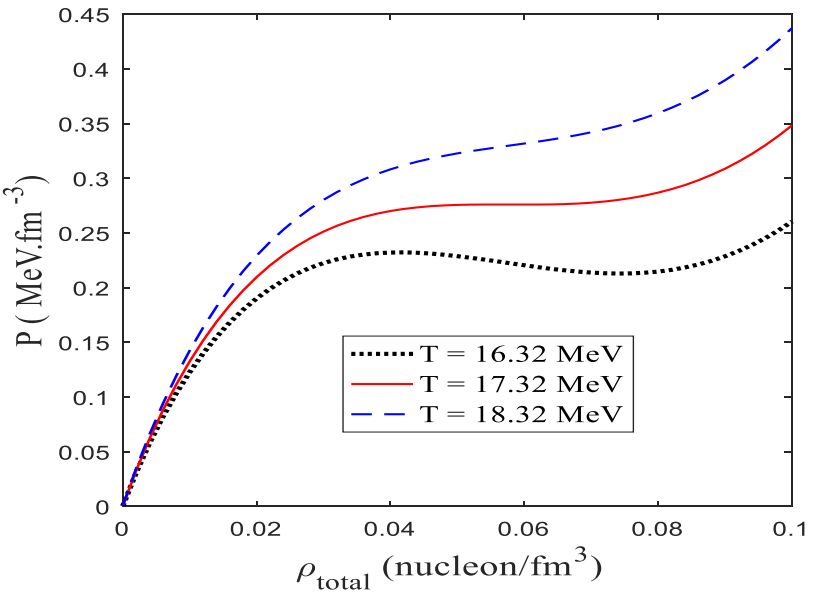

Fig. 3.3: Pressure isotherms for a nucleonic gas with the Skyrme interaction ($\boldsymbol{\sigma = 0.25}$) at the critical temperature 17.32 MeV and at two nearby temperatures.

In order to determine the critical temperature, we plot several isotherms at different temperatures differing by 1 MeV. We can conclude that the critical temperature for a nucleonic gas with Skyrme interactions ($\sigma = 0.25$) is 17.32 MeV as illustrated in Fig. 3.3. Hence the critical point for an infinite symmetric nuclear matter consists of nucleons interacting via Skyrme interaction is defined in table 3.2.

Table 3.2: The critical point for symmetric nuclear matter with including Skyrme interaction at different temperatures with $\boldsymbol{\sigma = 0.25}$.

	$T_{critical}$ (MeV)	$\rho_{critical}$ (nucleon/fm^3)	$P_{critical}$ (MeV.fm^{-3})
In this work	17.32	0.058	0.2759
H. R. Jaqaman [3]	17.34	-	-
S. Levit, and P. Bonche [14]	17.22	0.057	0.27
S. Talahmeh, and H. R. Jaqaman [18]	17.3	-	-

The small difference between our result and other ones may be attributed to the different number of terms (n) included in the pressure isotherm series as defined in Eq. 3.14. In [3] the series summation of pressure was carried up to n = 5 whereas in [14] the summation involved the terms n = 1 only. On the other hand, in [18] and our work the pressure series was summed up to n = 6.

CHAPTER 4

NUCLEAR STATISTICAL EQUILIBRIUM MODEL (NSE)

The nuclear matter vapour phase becomes inhomogeneous due to the existence of light clusters at moderate temperatures and densities much less than the saturation density. These clusters which are classified as bound nuclear states can minimize nuclear matter energy. Moreover, these two-, three-, and many-body correlations will change nuclear matter composition and modify its thermo-dynamical behaviour. At $\rho \ll 0.17$ nucleon/fm^3 with moderate temperatures $T \leq 20$ MeV, an effective interaction potential expresses the nucleon-nucleon interaction and the quark substructure and excitations of internal degrees of freedom of nucleons are neglected [7].

Nuclear matter with clusters is widely discussed in many studies which depend on several theoretical investigations, they showed that clusters are dominant at very low densities and must be included in the nuclear matter equation of state.

4.1 CLUSTERED NUCLEAR MATTER THEORETICAL INVESTIGATIONS

Including clusters in the nuclear matter equation of state has been studied by using various models; each one treats nuclear matter with a different technique than the others.

4.1.1 THE VIRIAL EXPANSION

This model is one of the oldest and general methods in constructing the equation of state of a dilute gas. Bound and scattering states are included here, but the medium effects on the cluster formation and dissolution are neglected.

It has two major assumptions. First, a gas phase system with decreasing temperature or increasing density does not undergo a phase transition. Second, fugacity ($z = e^{\mu/T}$) is small, so the partition function can be expressed in powers of z. Here μ is the chemical potential and T is the temperature [6, 29].

4.1.2 THE MICROSCOPIC QUANTUM STATISTICAL APPROACH

The microscopic quantum statistical approach is a non-relativistic approach based on the many body theory. It uses effective nucleon-nucleon interactions explicitly and includes the medium effects on the cluster formation and dissolution. It treats the nucleons and clusters as quasi-particles. The quasi-particle energy of a cluster consisting of A-nucleons (Z protons and N neutrons) in the ground state is given by [7, 13, 30]:

$$E_{A,Z}^{quasi}(k) = E_{A,Z}^{0} + \frac{k^2}{2\,A\,m} + \Delta E_{A,Z}^{SE}(k) + E_{A,Z}^{Pauli}(k) + \Delta E_{A,Z}^{Coulomb}(k) + \cdots \quad (4.1)$$

where m is the nucleon mass, and k is the cluster's momentum. The first term in Eq. 4.1 expresses the cluster binding energy in vacuum, while the second one is the cluster's kinetic energy. $\Delta E_{A,Z}^{SE}(P)$ is the shift that occurs in the self-energy due to the

medium effects, where the self-energy is the potential felt by the cluster including all interactions between the cluster and all other clusters and free nucleons. $E_{A,Z}^{Pauli}(P)$ is the Pauli blocking term which will be discussed later in this chapter. Finally, $\Delta E_{A,Z}^{Coulomb}(P)$ is the Coulomb term, it expresses the cluster energy change due to the electric repulsion between the cluster's protons. However, it is small and vanishes as we switch off the Coulomb force in symmetric nuclear matter.

4.1.3 RELATIVISTIC MEAN FIELD MODEL (RMF)

The clusters are treated as point-like particles and their internal structure is neglected. Nucleons interact by mesons exchange between them [7, 31].

The medium-modified clusters are inserted as explicit degrees of freedom and treated as quasi-particles. The medium effects are included by using density and temperature-dependent shifts of cluster binding energy.

4.1.4 NUCLEAR STATISTICAL EQUILIBRIUM MODEL (NSE)

The Nuclear Statistical Equilibrium is the simplest model that treats nuclear matter from a statistical point of view [4, 32]. My work is built on it with some modifications.

4.2 NUCLEAR STATISTICAL EQUILIBRIUM MODEL (NSE) IN ORIGINAL FORM

The Nuclear Statistical Equilibrium model treats the nuclear matter at low densities from a statistical point of view as non-interacting or minimally interacting particles at statistical equilibrium. Bound states are just included here while the excited and scattering states are ignored as are the medium modifications [7]. All models should reproduce the limiting cases of the NSE model at very low densities.

In this work we will deal with Low Density Clustered Symmetric Nuclear Matter that consists of fermions (free nucleons and fermionic clusters – odd mass number) and bosons (bosonic clusters – even mass number). The effective nucleon-nucleon interaction is ignored here since we don't want to double-count the effect of the interaction; the clusters are formed as a result of the interaction between nucleons.

Each cluster type has its own mass number (A = N + Z) in clustered symmetric nuclear matter, these clusters are in chemical equilibrium with the surrounding nucleons in the vapour as NSE model assumes.

$$\mu_{cluster} = Z\,\mu_p + N\,\mu_n = A\,\mu \tag{4.2}$$

where $\mu_{cluster}$ and μ are the chemical potential for the cluster and the surrounding vapour of nucleons respectively. Here the proton and neutron chemical potentials are equal ($\mu_p = \mu_n$) due to the properties of symmetric nuclear matter. The nucleon's chemical potential is given by Eq. 2.2. The total density of clustered symmetric

nuclear matter consists of all contributions from free nucleons and clusters, which is given by

$$\rho_{total} = \rho_{free\ nucleons} + \sum A_{cluster}\,\rho_{cluster} \tag{4.3}$$

The contribution of each type of cluster to the total density depends on the probability ($n_{cluster}$) of finding the cluster in its ground state with kinetic energy $\varepsilon^0_{cluster} = \frac{\hbar^2 k^2}{2\,m_{cluster}}$ and its spin degeneracy factor ($g = 2s + 1$ where s is the cluster's spin) [18, 33].

$$\rho_{cluster} = \frac{g}{(2\pi)^3}\int d^3k\, n_{cluster} \tag{4.4}$$

$$n_{cluster} = \{exp[\beta(\varepsilon^0_{cluster} - \mu_{cluster} - B^0_{cluster}) \pm 1]\}^{-1} \tag{4.5}$$

where the $(+)$ sign is used for fermionic clusters while the $(-)$ sign is used for bosonic clusters. $B^0_{cluster}$ is the cluster's binding energy at zero density, that is in vacuum.

The original NSE model predicts that at high density most nucleons in symmetric nuclear matter would be bound and form different clusters. However, this is unphysical and can be corrected by including the medium effects on cluster formation and dissolution.

In this work, we will modify the NSE and take into account the medium effects to remedy its deficiency by considering the reduction in the binding energy of the clusters as the density of the surrounding vapour increases.

4.3 THE MODIFIED NUCLEAR STATISTICAL EQUILIBRIUM MODEL

Clusters dissolve as clustered symmetric nuclear matter density increases. The main medium effect is called the Pauli blocking which is caused by the fermionic nature of nucleons (protons and neutrons) where the quantum mechanics treat them as indistinguishable particles and requires the total wavefunction to be anti-symmetric under the exchange of any two identical fermions. This leads to the Pauli Exclusion Principle which prevents identical particles from occupying the same point in the position and momentum phase-space simultaneously. This applies not only to the exchange of nucleons inside a cluster but also to the exchange of any of these nucleons with the free nucleons in the outside vapour.

Pauli blocking acts on the bound states (clusters) by decreasing their binding energy as the density of symmetric nuclear matter increases [7, 30, 34]. At a certain point in medium density, the binding energy of the cluster vanishes and the cluster dissolves to its constituents. This point is known as the Mott density ρ_{Mott} [13]. Each cluster has its characteristic Mott density which depends on its temperature and its centre of mass momentum. The cluster can survive to higher densities as temperature increases or if it has non-zero CM momentum (that is the Mott density increases with

temperature) [35]. In this work, we will use Mott densities calculated at zero CM momentum clusters [7].

4.3.1 DENSITY-DEPENDENT BINDING ENERGY

The modification that we entered to NSE model to remedy its insufficiency is to use a density-dependent binding energy for the cluster which we must include in Eq.4.5 instead of the binding energy at zero-density, that is the binding energy of the corresponding nucleus with the same A and Z. The binding energies of light clusters we use were calculated in [7]. They decrease almost linearly with density and to simulate these effects we have used the following form:

$$B_{Cluster} = B^{0}_{cluster}\left(1 - \frac{\rho_{total}}{\rho_{Mott}}\right) \qquad (4.6)$$

4.3.2 MOTT DENSITY OF CLUSTERS

The medium effects on the cluster's binding energy were studied by using different models [30, 36]. To get zero CM momentum Mott densities for our clusters we used the results of Typel et al [7] which were based on the relativistic mean field model (RMF) which are shown in Fig. 4.1. The values of the Mott densities up to A = 4 obtained from these results are listed in table 4.1.

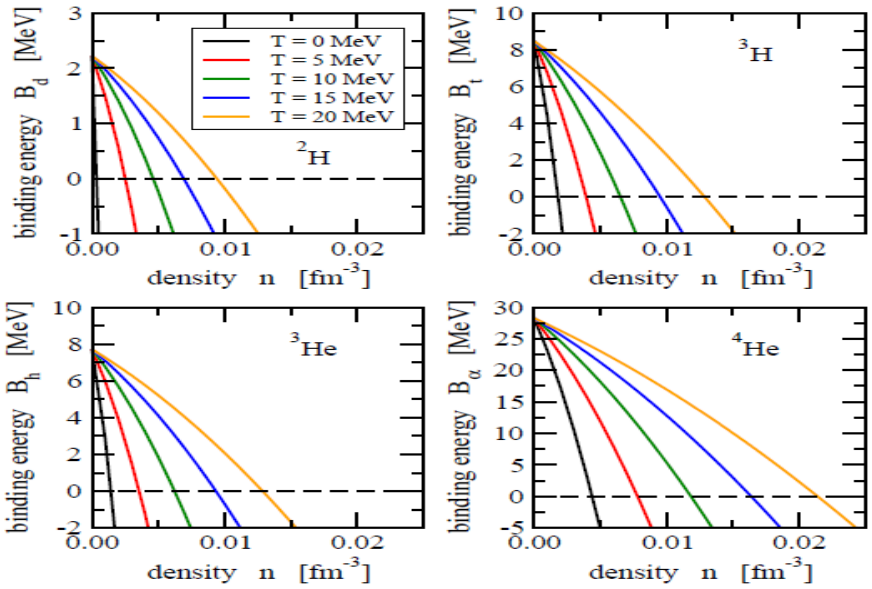

Fig. 4.1: The binding energy as a function of medium density for deuteron, triton, helion and alpha clusters at different temperatures [7].

Table 4.1: Zero-CM momentum Mott density values for deuteron, triton, helion and alpha clusters at different temperatures.

	T = 5 MeV	T = 10 MeV	T = 15 MeV	T = 20 MeV
Deuteron [nucleon/fm^3]	0.0025	0.0047	0.0071	0.0095
Triton [nucleon/fm^3]	0.0040	0.0065	0.0096	0.0129
Helion [nucleon/fm^3]	0.0035	0.0063	0.0094	0.0128
Alpha [nucleon/fm^3]	0.0080	0.0120	0.0165	0.0215

The Mott densities for heavier clusters (A > 4) can be extrapolated from the Mott densities for the deuteron, triton, helion and alpha clusters $(d, t, h\ and\ \alpha)$ at different temperatures. First we use a quadratic polynomial fit method to parameterize the Mott densities for each cluster $(d, t, h\ and\ \alpha)$ as a function of temperature T.

$$Mott - density_i(T) = a\,T^2 + b\,T + c \qquad (4.7)$$

Where i is cluster indicator and (a, b and c) are the coefficients of the quadratic polynomial which are listed in table 4.2.

Table 4.2: Temperature-dependant Mott densities Quadratic polynomial coefficients for $(\boldsymbol{d, t, h\ and\ \alpha})$.

Cluster	a $\left[\frac{\text{nucleon}}{\text{fm}^3\ \text{MeV}^2}\right]$	b $\left[\frac{\text{nucleon}}{\text{fm}^3\ \text{MeV}}\right]$	c $\left[\frac{\text{nucleon}}{\text{fm}^3}\right]$
Deuteron	0.004958	0.000418	0.00035
Triton	0.01983	0.000396	0.0018
Helion	0.0148725	0.00047	0.001
Alpha	0.0067379	0.00065	0.0045

So at any temperature, we can know the extrapolated Mott densities for $(d, t, h\ and\ \alpha)$ clusters.

Secondly, for each temperature, Mott densities for heavier clusters can be estimated by extrapolating the Mott densities of these four light clusters using a quadratic fit polynomial method

$$Mott - density\ (A) = p\ A^2 + q\ A + r \tag{4.8}$$

The coefficients $(p, q\ and\ r)$ are listed in table 4.3 for different temperatures. These coefficients are obtained by fitting the Mott densities of the four light clusters with (A < 5). An example of this extrapolation procedure at T = 6 MeV is shown in Fig. 4.2.

Table 4.3: Quadratic polynomial coefficients for mass number-dependant Mott densities at different temperatures.

	p [nucleon^{-1} fm^{-3}]	q [fm^{-3}]	r [nucleon fm^{-3}]
T = 2 MeV	0.0012	−0.0049	0.0062
T = 4 MeV	0.00145	− 0.0061	0.0085
T = 6 MeV	0.0016	−0.00665	0.0098
T = 8 MeV	0.00175	−0.00725	0.0113
T = 10 MeV	0.0019	−0.00775	0.0126
T = 12 MeV	0.0021	−0.0086	0.0145

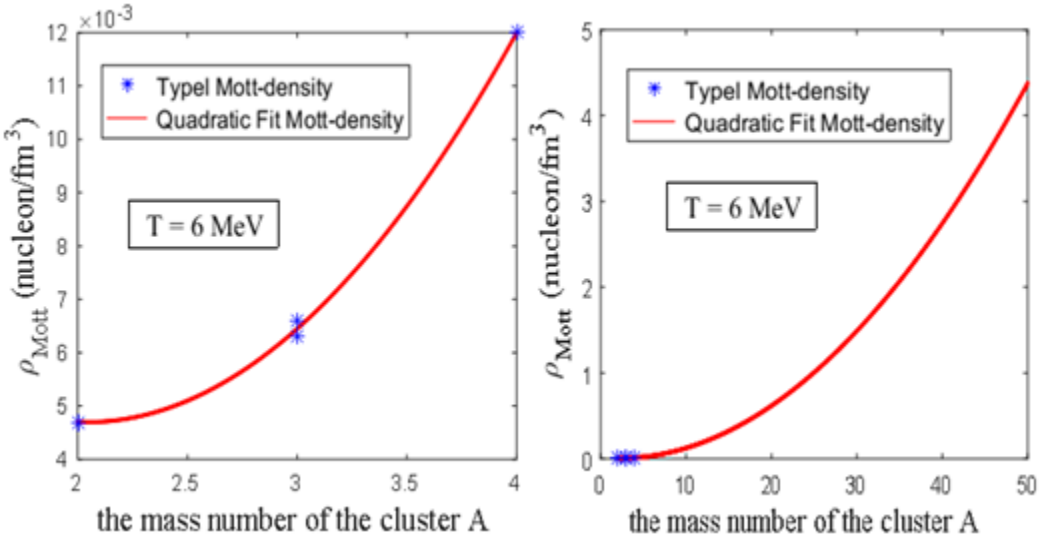

Fig. 4.2: Mott density as a function of mass number at T = 6 MeV.

CHAPTER 5

CLUSTERED SYMMETRIC NUCLEAR MATTER

The composition of clustered symmetric nuclear matter can be determined by evaluating the fraction $X_{cluster}$ of nucleons that are consumed in building each type of clusters:

$$X_{cluster} = A_{cluster} \frac{\rho_{cluster}}{\rho_{total}} \tag{5.1}$$

where $\rho_{cluster}$ and ρ_{total} are given by Eq. 4.4 and Eq. 4.3 respectively.

Now, we are ready to study the abundance of clusters at different temperatures. But there is still one problem related to the strength of the two body correlations which is called the Deuteron abundance overestimation. This problem had been studied in [7, 36]. They found that deuterons can be formed only for CM momenta larger than the deuteron Mott momentum $\hbar k_d^{Mott}$ if symmetric nuclear matter densities are higher than the Deuteron Mott density. However, this has a strong effect on the fractions of other clusters. So to avoid this problem, they suggested that we must limit our momenta only over the region $k > k_d^{Mott}$ where the bound state energy is lower than the continuum of scattering states. These corrections become important with increasing temperatures.

The value of k_d^{Mott} as calculated in [29] is given by:

$$\left[k_d^{Mott}\left(T\,, \rho_{total}\,, \rho_{Mott,d} \right)\right]^2$$

$$\approx \left\{ \begin{array}{c} \dfrac{-\left(4.5185-0.16164\,T+0.0056582\,T^2\right)}{2\,\left(1.32-0.02782\,T\right)} \\ + \left[\dfrac{\left(4.5185-0.16164\,T+0.0056582\,T^2\right)^2}{4(1.32-0.02782\,T)^2} + \dfrac{1000\,\left(\rho_{total}-\,\rho_{Mott,d}\right.}{\left(1.32-0.02782\,T\right)}\right]^{1/2} \end{array} \right\} \qquad (5.2)$$

The effect of limiting the deuteron momenta integration to the region $k > k_d^{Mott}$ is shown in Fig. 5.1 below. This overestimation appears only in the case of the deuteron because of its extremely low binding energy.

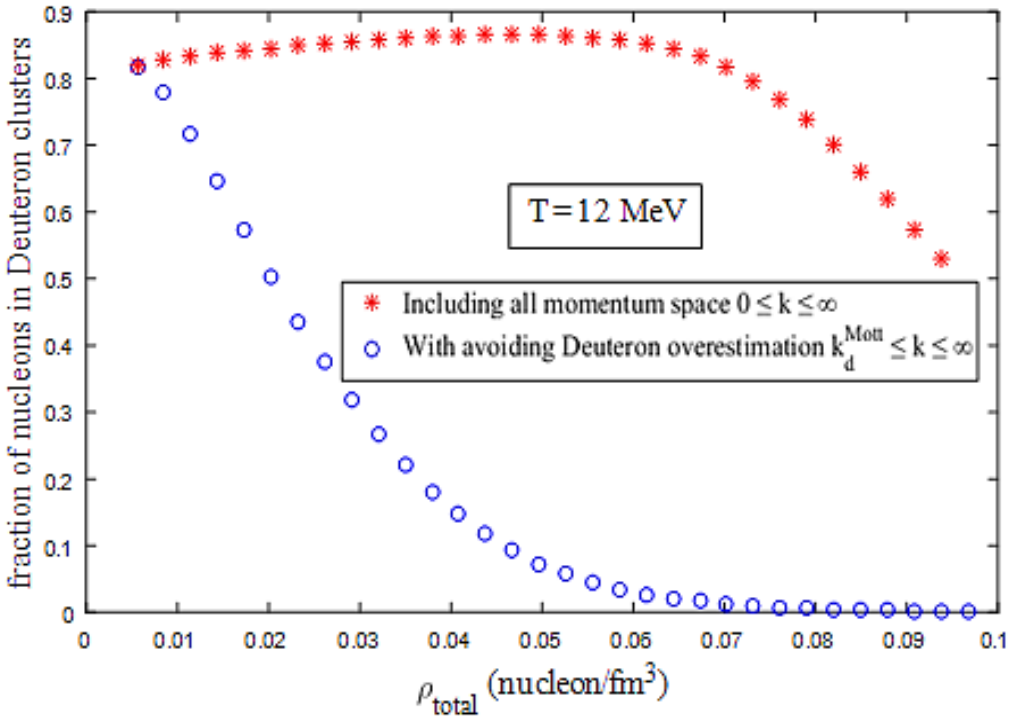

Fig. 5.1: Fraction of nucleons in Deuteron clusters with including all momentum space and with case of avoiding Deuteron overestimation at T = 12 MeV.

5.1 CLUSTERS INCLUDED IN THIS WORK

Most previous studies [7, 16, 37] examined clusterization in nuclear matter by including deuteron, triton, helion and alpha clusters and established its equation of state by using different approaches. Moreover, there are few studies which included more clusters like [17] which included clusters with mass number up to A = 13 and [19] which included clusters with mass number up to A = 25. In this work, we included light and medium nuclei with mass number up to A = 50. For each A the nucleus which has the largest binding energy per nucleon is selected. In addition, for each collection of isobars we also selected and included in the calculation any other isobar whose binding energy per nucleon differs by no more than 0.1 MeV from the nucleus with the highest B/A. In total 89 clusters were thus selected and included in our equation of state. They are listed in table 5.1.

Table 5.1: The binding energies, spin, spin-degeneracy factor and mass of the nuclei used in the present calculation [38].

Cluster	A	$B/A(MeV)$	$B^0_{cluster}\ (MeV)$	Spin	g	Mass (MeV/c^2)
H	2	1.112283	2.224566	1	3	1875.612929
H	3	2.827266	8.481798	0.5	2	2808.921109
He	3	2.572681	7.718043	0.5	2	2808.39158
He	4	7.073915	28.29566	0	1	3727.379375

He	5	5.481	27.405	1.5	4	4667.831413
Li	6	5.332345	31.99407	1	3	5601.518569
Li	7	5.606291	39.244037	1.5	4	6533.834014
Be	8	7.062435	56.49948	0	1	7454.850833
Be	9	6.46276	58.16484	1.5	4	8392.750907
Be	10	6.49771	64.9771	0	1	9325.50401
B	10	6.47507	64.7507	3	7	9324.437375
B	11	6.92771	76.20481	1.5	4	10252.54866
C	12	7.680144	92.161728	0	1	11174.8642
C	13	7.469849	97.108037	0.5	2	12109.4833
C	14	7.520319	105.284466	0	1	13040.87228
N	14	7.475614	104.658596	1	3	13040.20527
N	15	7.699459	115.491885	0.5	2	13968.93739
O	16	7.976206	127.619296	0	1	14895.08261
O	17	7.750731	131.762427	2.5	6	15830.50489
O	18	7.76703	139.80654	0	1	16762.02628
F	19	7.779015	147.801285	0.5	2	17692.30419

Ne	20	8.03224	160.6448	0	1	18617.73353
Ne	21	7.971713	167.405973	1.5	4	19550.53778
Ne	22	8.080465	177.77023	0	1	20479.73894
Na	23	8.111493	186.564339	1.5	4	21409.2178
Mg	24	8.260709	198.257016	0	1	22335.79821
Mg	25	8.223504	205.5876	2.5	6	23268.03305
Mg	26	8.333872	216.680672	0	1	24196.50539
Mg	27	8.263854	223.124058	0.5	2	25129.62742
Al	27	8.331545	224.951715	2.5	6	25126.50757
Si	28	8.447744	236.536832	0	1	26053.19581
Si	29	8.448634	245.010386	0.5	2	26984.28766
Al	29	8.34872	242.11288	2.5	6	26988.47705
Si	30	8.520653	255.61959	0	1	27913.24387
P	31	8.481178	262.916518	0.5	2	28844.22043
Si	31	8.45829	262.20699	1.5	4	28846.22189
S	32	8.493134	271.780288	0	1	29773.63027
Si	32	8.481569	271.410208	0	1	29776.58408

P	32	8.46413	270.85216	1	3	29775.85019
S	33	8.497634	280.421922	1.5	4	30704.55407
P	33	8.51381	280.95573	0.5	2	30705.31198
S	34	8.583501	291.839034	0	1	31632.70237
Cl	35	8.520278	298.20973	1.5	4	32564.60542
P	35	8.44625	295.61875	0.5	2	32569.77994
S	35	8.537854	298.82489	1.5	4	32565.2819
Ar	36	8.519909	306.716724	0	1	33494.37236
S	36	8.575387	308.713932	0	1	33494.95828
Cl	36	8.521927	306.789372	2	5	33495.59119
Cl	37	8.57028	317.10036	1.5	4	34424.84562
Ar	37	8.527139	315.504143	1.5	4	34425.15034
Ar	38	8.614273	327.342374	0	1	35352.87754
K	39	8.55702	333.72378	1.5	4	36284.77017
Cl	39	8.4944	331.2816	1.5	4	36289.79517
Ar	39	8.56259	333.94101	3.5	8	36285.84396
Ca	40	8.551301	342.05204	0	1	37214.71615

Ar	40	8.595259	343.81036	0	1	37215.54039
K	40	8.538083	341.52332	4	9	37216.53608
K	41	8.576061	351.618501	1.5	4	38146.0063
Ar	41	8.534371	349.909211	3.5	8	38149.0069
Ca	41	8.546703	350.414823	3.5	8	38145.91876
Ca	42	8.616559	361.895478	0	1	39074.00354
Ar	42	8.55561	359.33562	0	1	39079.14604
K	42	8.551245	359.15229	2	5	39078.03791
Ca	43	8.600659	369.828337	3.5	8	40005.63605
K	43	8.57663	368.79509	1.5	4	40007.96075
Sc	43	8.53082	366.82526	3.5	8	40007.34812
Ca	44	8.65817	380.95948	0	1	40934.07037
Sc	45	8.61884	387.8478	3.5	8	41865.4564
K	45	8.55451	384.95295	1.5	4	41870.93311
Ca	45	8.63054	388.3743	3.5	8	41866.22098
Ti	45	8.555631	385.003395	3.5	8	41867.00991
Ti	46	8.656356	398.192376	0	1	42793.38638

Ca	46	8.66889	398.76894	0	1	42795.39193
Sc	46	8.621922	396.608412	4	9	42796.26119
Ti	47	8.661121	407.072687	2.5	6	43724.07147
Ca	47	8.63926	406.04522	3.5	8	43727.68096
Sc	47	8.66499	407.25453	3.5	8	43725.18027
V	47	8.582127	403.359969	1.5	4	43726.49339
Ti	48	8.722903	418.699344	0	1	44652.01024
Ca	48	8.66647	415.99056	0	1	44657.30089;8
Sc	48	8.65604	415.48992	6	13	44656.50995
V	48	8.62301	413.90448	4	9	44655.51418
Ti	49	8.711055	426.841695	3.5	8	45583.43326
Sc	49	8.68607	425.61743	3.5	8	45585.94824
V	49	8.682806	425.457494	3.5	8	45583.52672
Cr	49	8.61327	422.05023	2.5	6	45585.64495
Cr	50	8.700981	435.04905	0	1	46512.21005
Ti	50	8.755618	437.7809	0	1	46512.05947
V	50	8.695869	434.79345	6	13	46513.75622

5.2 CLUSTERED SYMMETRIC NUCLEAR MATTER COMPOSITION AT DIFFERENT TEMPERATURES

In this section, the composition of symmetric nuclear matter at each temperature was determined separately. First, 25 clusters were included just as in a previous study [19] to compare the results of the two studies and to notice the effect of including more clusters on the composition of symmetric nuclear matter. Second, clusters with mass number up to A= 50 were included and the fraction of nucleons in each type of cluster was estimated at different temperatures. At each Temperature the composition of clustered symmetric nuclear matter is determined as a function of total nuclear matter density up to 0.1 nucleon/fm^3.

5.2.1 CLUSTERED SYMMETRIC NUCLEAR MATTER AT T = 2 MeV

The composition of clustered symmetric nuclear matter at T = 2 MeV is shown in Fig. 5.2 and Fig. 5.3. At T = 2 MeV as special case, for each figure the density range was separated to get the obvious changes in the composition of clustered symmetric nuclear matter which occur in this case at extremely low densities as compared with our upper density limit of 0.1 nucleon/fm^3.

At densities less than 0.0016 nucleon/fm^3 clusters with mass number up to A = 5 are dominant regardless of what heavier clusters are included in symmetric nuclear matter as illustrated in Fig. 5.2 and Fig. 5.3.a. These are mostly alpha particles as

shown later in the next subsection. However, as the densities increase the presence of heavier clusters becomes more important.

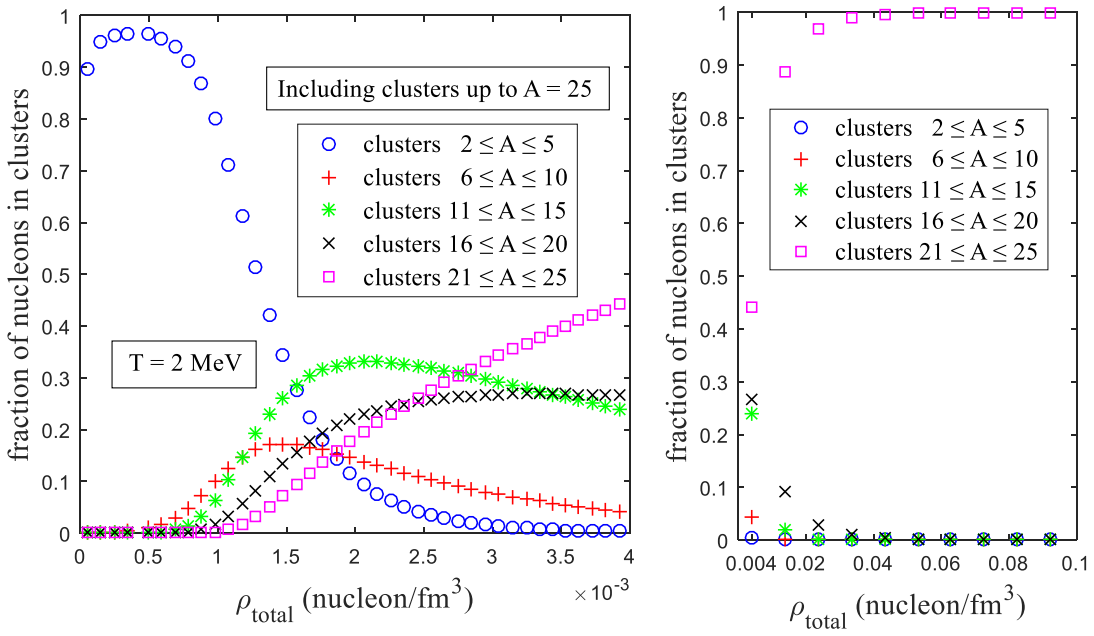

Fig. 5.2: Clustered symmetric nuclear matter composition at T = 2 MeV when the calculation included clusters up to A = 25 only.

In the first case as illustrated in Fig. 5.2 when only clusters up to A = 25 were included, the fraction of nucleons in clusters with mass number $(6 \leq A \leq 10)$ does not exceed 16% and has its largest fraction in the density range (0.001 – 0.003) nucleon/fm^3. However, clusters with mass number $(11 \leq A \leq 15)$ are the dominant clusters in symmetric nuclear matter in the density range (0.0016 – 0.0027) nucleon/fm^3. For the whole density range, the fraction of nucleons in clusters with mass number $(16 \leq A \leq 20)$ does not exceed 27%. At $\rho = 0.001$ nucleon/fm^3,

clusters with mass number ($21 \leq A \leq 25$) start to form and become the dominant clusters at $\rho \geq 0.003$ nucleon/fm^3 and the lighter clusters almost disappear for densities higher than $\rho = 0.039$ nucleon/fm^3. The contribution of the heaviest fragments ($21 \leq A \leq 25$) becomes almost 100% for $\rho > 0.004$ nucleon/fm^3. As seen in Fig. 5.3.b this unrealistic result changes when we include more clusters in the calculation.

Now, by including the 89 clusters in symmetric nuclear matter the fraction of nucleons in clusters with mass number ($A \leq 25$) at $\rho \geq 0.002$ nucleon/fm^3 does not exceed 35% due to the formation of other clusters with mass number ($25 \leq A \leq 50$). However, clusters with mass number ($A \geq 26$) start to form at $\rho = 0.0012$ nucleon/fm^3. Clusters with mass number ($31 \leq A \leq 35$) are dominant in the density range 0.0027 - 0.008 nucleon/fm^3 although their fraction does not exceed 25%. After that, the dominant clusters are those with mass number ($46 \leq A \leq 50$) up to 0.1 nucleon/fm^3 as shown in Fig. 5.3.b. In particular we note that the percentage of nucleons in one group of clusters never reaches 100% when we include the clusters ($A > 25$) in the calculation.

In the present work we included several isobars for each A. For example the mass number range 46 – 50 has 18 different nuclides and the range 41 – 50 has 14 different nuclides. So when the fraction of heaviest clusters group ($46 \leq A \leq 50$) reaches 90% at 0.1 nucleon/fm^3 which is about 5% per cluster type whereas The fraction of heaviest clusters group ($21 \leq A \leq 25$) reaches 100% when we included only clusters

up to A = 25 which has only five different nuclides that means each cluster type had an unrealistically large contribution of 20% per cluster.

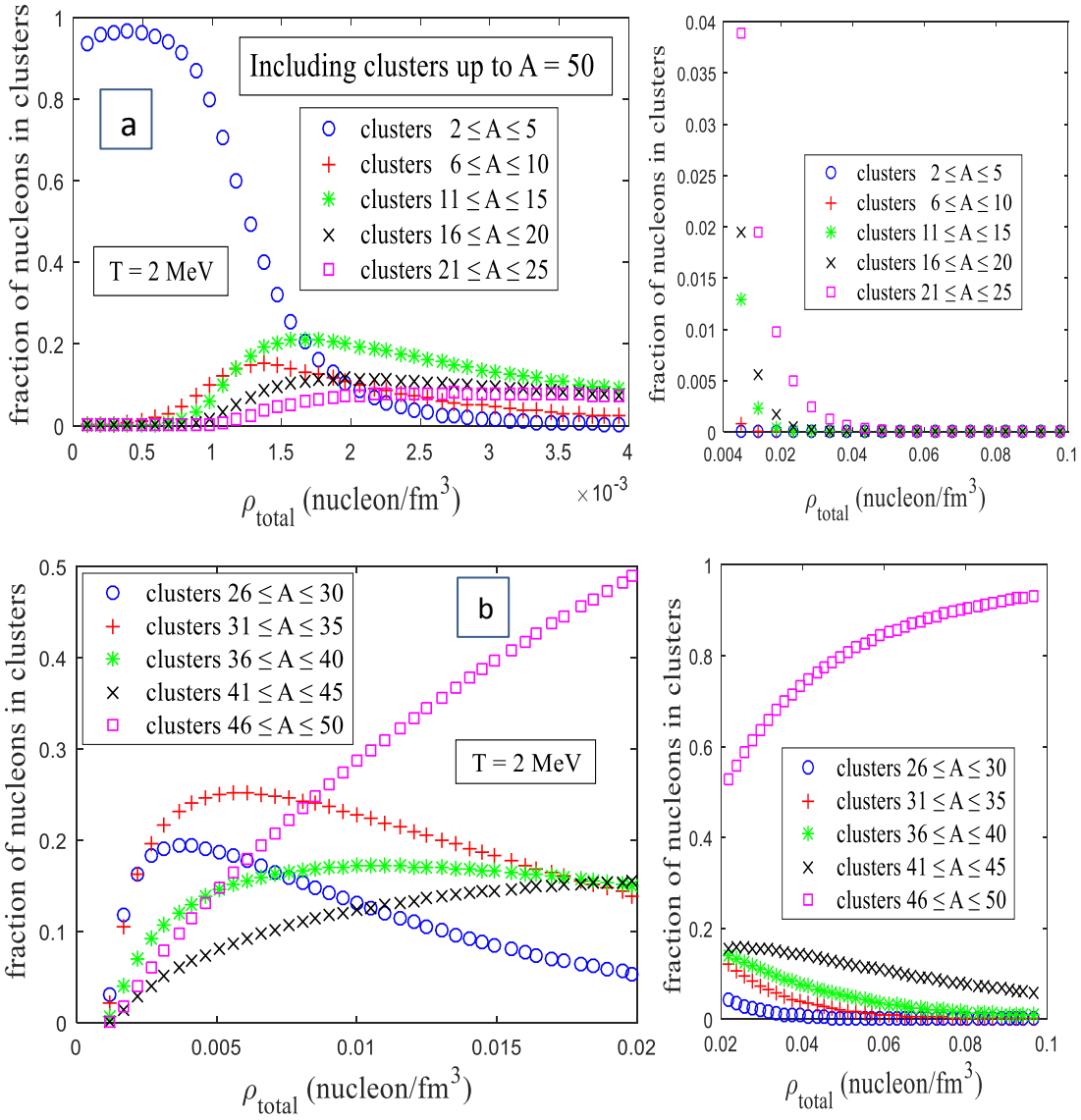

Fig. 5.3: Clustered symmetric nuclear matter composition at T = 2 MeV by including clusters with mass number up to A = 50 in the calculation. The upper part (a) represents the fraction of nucleons in clusters with mass number $2 \leq A \leq 25$, whereas the lower part (b) represents the fraction of nucleons in clusters with mass number $26 \leq A \leq 50$.

5.2.2 CLUSTERED SYMMETRIC NUCLEAR MATTER AT T = 4 MeV

The cluster fractions in symmetric nuclear matter at T = 4 MeV as a function of the total density are given in Fig. 5.4 when clusters up to A = 25 only were included in the clustered symmetric nuclear matter and in Fig. 5.5 when clusters up to A = 50 were included. At densities less than 0.005 nucleon/fm^3 clusters with mass number up to A = 5 are dominant irrespective of what clusters are included in symmetric nuclear matter. These light clusters up to A = 5 are mainly deuterons as shown in Fig. 5.6. In particular 61% of nucleons are bound in theses clusters at 0.005 nucleon/fm^3 and the percentage is higher at lower densities reaching a maximum of about 91%. On the other hand, this fraction decreases with increasing density and they disappear completely at densities of about 0.014 nucleon/fm^3 because of the dissolution of these clusters due to their low Mott densities and the formation of heavier clusters.

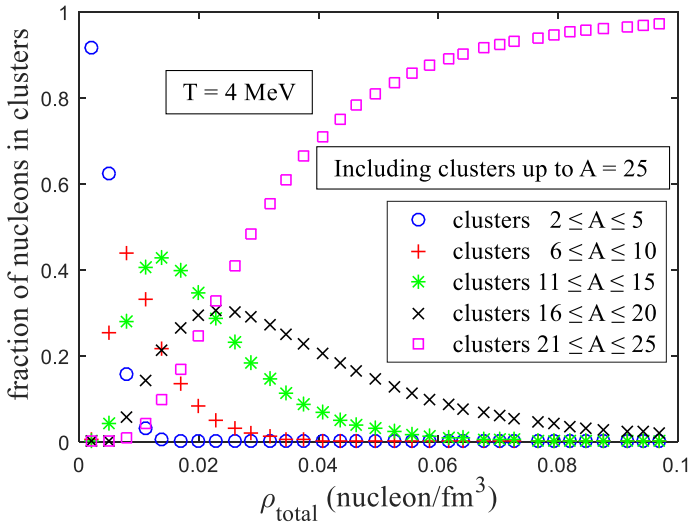

Fig. 5.4: Clustered symmetric nuclear matter composition at T = 4 MeV when the calculation included clusters up to A = 25 only.

In both cases regardless of what heavier clusters are included in the calculations, as the fraction of the lightest clusters goes down, clusters with mass number ($6 \leq A \leq 10$) appear strongly with a fraction that reaches a maximum of 44% at a density around 0.008 nucleon/fm^3. With almost the same maximum fraction but at 0.012 nucleon/fm^3, nucleons are bound in clusters with mass number ($11 \leq A \leq 15$). However, the fraction of nucleons in clusters with mass number ($16 \leq A \leq 20$) does not exceed 30% along the whole density range when clusters up to A = 25 only were included in the calculations and this fraction is reduced to 22% when the 89 clusters were included.

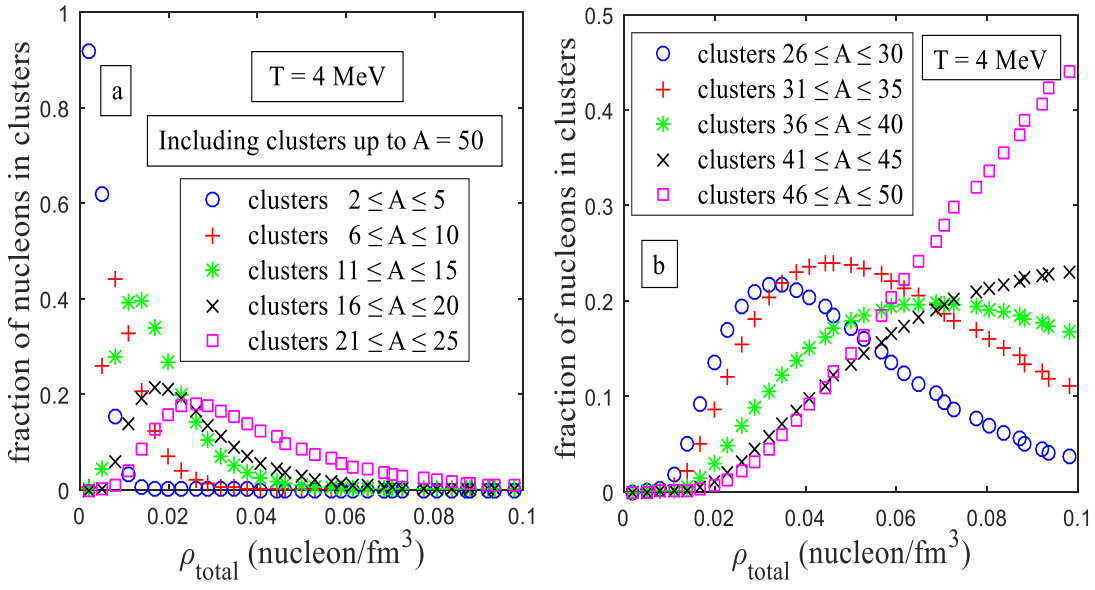

Fig. 5.5: Clustered symmetric nuclear matter composition at T = 4 MeV. The left part (a) gives the fraction of nucleons in clusters up to A = 25 when the clusters up to A = 50 were included in the calculations, whereas the right part (b) gives the fraction of nucleons in clusters with 26 < A < 50.

As shown in Fig. 5.4, clusters with mass number $(21 \leq A \leq 25)$ appear strongly at density 0.023 nucleon/fm^3 and remain dominant up to 0.1 nucleon/fm^3 where their contribution reaches almost 100% when only clusters up to A= 25 are included in the calculation. However, when clusters up to A = 50 are included the fraction of nucleons in these clusters reaches its maximum of 18% at 0.026 nucleon/fm^3 before dying gradually due to the formation of clusters with mass number $(A \geq 25)$ which start to appear at 0.011 nucleon/fm^3 as displayed in Fig. 5.5.a.

At 0.062 nucleon/fm^3, clusters with mass number $(46 \leq A \leq 50)$ would have substantial contributions in symmetric nuclear matter and almost 40% of the system would consist of these clusters at 0.09 - 0.1 nucleon/fm^3. In particular, we note that the percentage of nucleons in this group of the heaviest clusters is well below 100% when we included the clusters with $(A > 25)$ in the calculation. The remaining bound nucleons are distributed among the different clusters in the range $(26 \leq A \leq 50)$. By including clusters up to A = 50 the heaviest clusters have a contribution of only 45% which is about 2.5% per cluster type .This behaviour is more realistic than what was obtained from the calculations with A up to 25 only, where the contribution of the heaviest clusters $(21 \leq A \leq 25)$ reaches almost 100% as can be seen from Fig 5.4 that means each cluster type had an unrealistically large contribution of 20%.

Deuterons are the two body correlations, so they are easily formed. So they are the dominant clusters at very low density but not at very low temperatures. In symmetric nuclear matter in the very low density region a large portion of nucleons are bound in

alpha particles at T ≤ 2MeV as illustrated in Fig. 5.6. At higher temperatures (T ≥ 4MeV), the deuterons become dominant but at T = 3MeV alphas still have a significant contribution at low densities as compared with deuterons. In particular, at very low temperature and density the cluster fractions are simply determined by the binding energies and alphas have a high binding energy per nucleon compared with other light clusters [39].

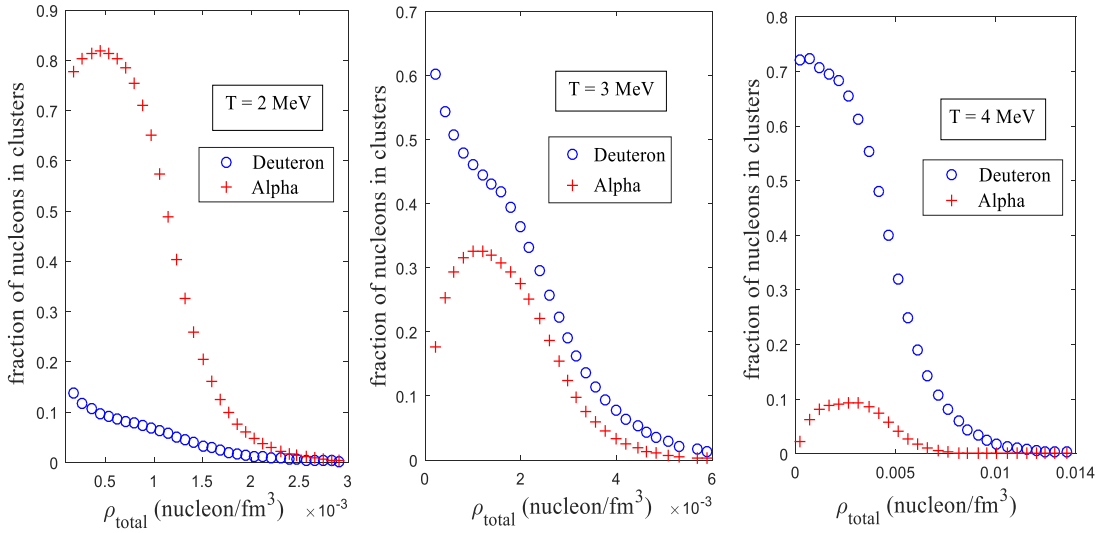

Fig. 5.6: Deuteron and alphas fractions in symmetric nuclear matter at T = 2 MeV, 3 MeV and 4 MeV.

5.2.3 CLUSTERED SYMMETRIC NUCLEAR MATTER AT T = 6 MeV

The composition of clustered symmetric nuclear matter at T = 6 MeV is shown in Fig. 5.7 and Fig. 5.8 which give the fraction of nucleons bound in each type of clusters as a function of total density. For very low densities up to 0.02 nucleon/fm^3 the composition of symmetric nuclear matter is still the same even if we included a

larger number of heavier clusters in the calculations. The significant differences occur in the fractions of clusters with mass number ($A \geq 16$), the fraction of nucleons in clusters with mass number ($16 \leq A \leq 20$) reaches 32% around 0.05 nucleon/fm^3 when we included only clusters up to A = 25 but with including the 89 clusters the fraction is reduced to 24% around 0.041 nucleon/fm^3.

On the other hand, clusters with mass number ($21 \leq A \leq 25$) become dominant after 0.05 nucleon/fm^3 in the first case when clusters up to A = 25 only were included in the symmetric nuclear matter. Whereas in the second case of including heavier clusters up to A = 50 the fraction of clusters with ($21 \leq A \leq 25$) along the whole density range does not exceed 21% and their contribution gradually decreases beyond 0.06 nucleon/fm^3.

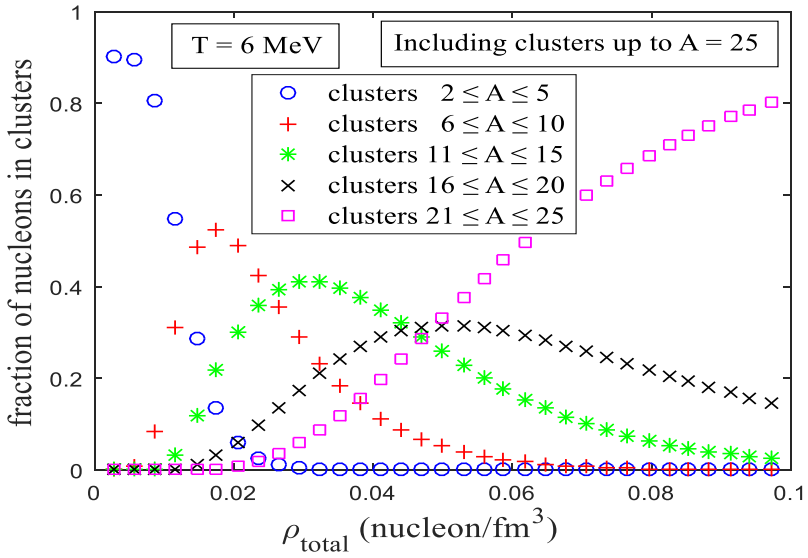

Fig. 5.7: Clustered symmetric nuclear matter composition at T = 6 MeV when the calculations included clusters up to A = 25 only.

When we included the 89 clusters in symmetric nuclear matter, the fraction of nucleons in each collection of clusters is shown in Fig. 5.8. Clusters with mass number up to 10 are dominant at $\rho \leq 0.02$ nucleon/fm^3. Whereas clusters with mass number $(11 \leq A \leq 20)$ appear strongly with fraction exceeds 50% at density range 0.026 – 0.049 nucleon/fm^3. However, 42% of nucleons are concentrated in clusters with mass number $(21 \leq A \leq 30)$ around 0.065 nucleon/fm^3. The remaining clusters strongly appear beyond 0.06 nucleon/fm^3 with fraction reaches to (29 – 65)%.

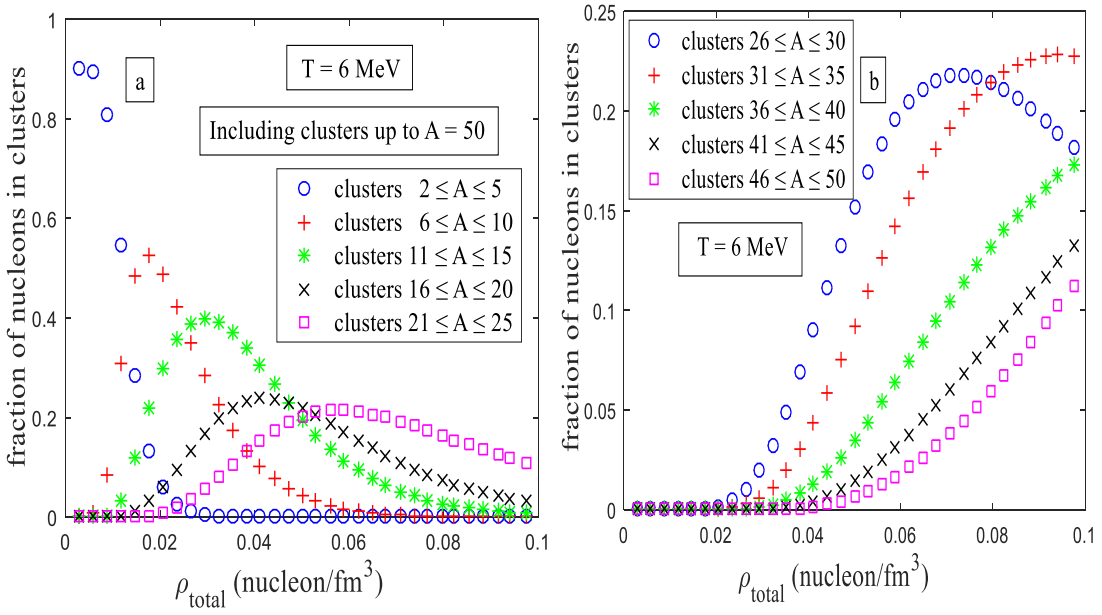

Fig. 5.8: Clustered symmetric nuclear matter composition at T = 6 MeV. The left part (a) represents the fraction of nucleons in clusters up to A = 25 when the clusters up to A = 50 were included in the calculations, whereas the right part (b) represents the fraction of nucleons in clusters 26 < A < 50.

5.2.4 CLUSTERED SYMMETRIC NUCLEAR MATTER AT T = 8 MeV

The composition of symmetric nuclear matter as a function of density at T = 8 MeV is shown in Fig. 5.9 and Fig. 5.10. Clusters with mass number $(2 \leq A \leq 10)$ are the dominant till 0.038 nucleon/fm^3 in symmetric nuclear matter regardless of other clusters that were included with fraction (90 – 50)%. Moreover, the fraction of nucleons in clusters with mass number $(11 \leq A \leq 15)$ has slight change between the first case of including clusters up to A = 25 and the second one of including clusters up to A = 50 in symmetric nuclear matter.

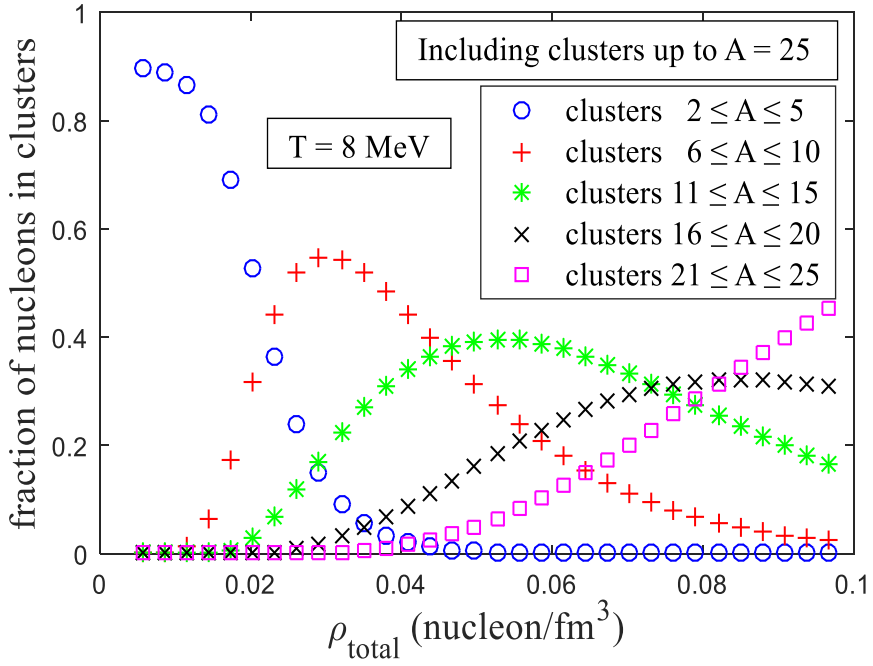

Fig. 5.9: Clustered symmetric nuclear matter composition at T = 8 MeV when the calculations included clusters up to A = 25 only.

The significant differences occur in the fractions of clusters with mass number ($A \geq 16$), the fraction of nucleons in clusters with mass number ($16 \leq A \leq 20$) reaches 32% around 0.08 nucleon/fm^3 if clusters up to A = 25 were included only in the calculations but with including the 89 clusters the fraction is reduced to 25% around 0.07 nucleon/fm^3. On the other hand, The fraction of nucleons in clusters with mass number ($21 \leq A \leq 25$) reaches 45% beyond 0.09 nucleon/fm^3 in the first case of including clusters up to A = 25 only. Whereas if we included more clusters up to A =50 in symmetric nuclear matter its fraction along the density range does not exceed 23%.

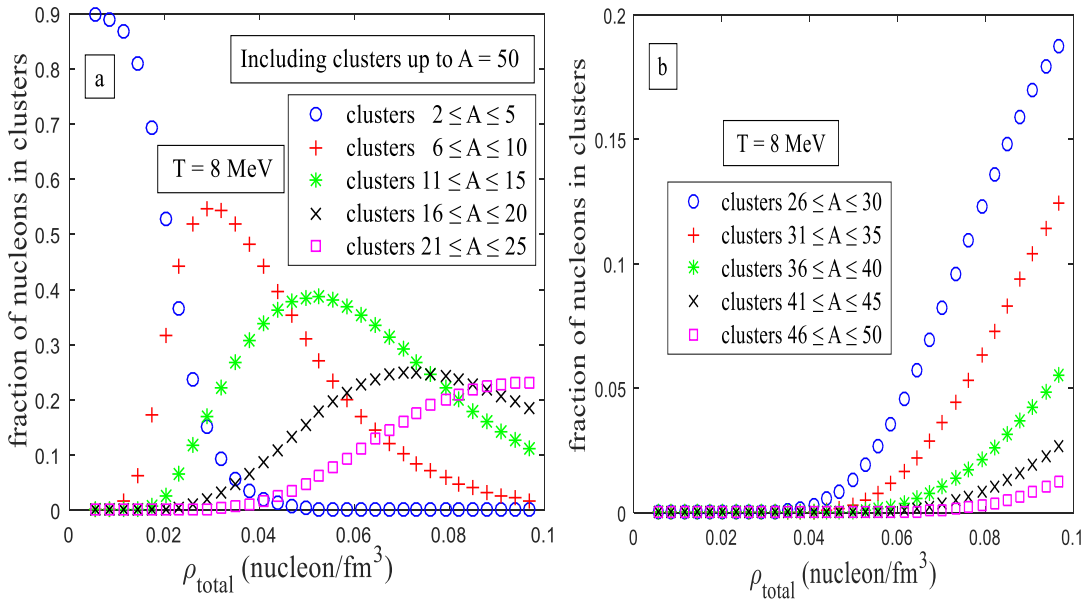

Fig. 5.10: Clustered symmetric nuclear matter composition at T = 8 MeV. The left part (a) represents the fraction of nucleons in clusters up to A = 25 when the clusters up to A = 50 were included in the calculations, whereas the right part (b) represents the fraction of nucleons in clusters 26 < A < 50.

In Fig. 5.10 we show the fraction of nucleons in each range of cluster size when we included the 89 clusters in our calculations for the composition of symmetric nuclear matter. At $\rho = 0.04$ nucleon/fm^3, the nucleons start gathering in clusters with mass number ($A \geq 26$) but their contribution remains small which reaches 42% at ρ = 0.1 nucleon/fm^3. So clusters with mass number up to A = 25 stays dominant up to ρ = 0.1 nucleon/fm^3 and they contribute about 76% of the nuclear matter at 0.08 nucleon/fm^3. These clusters appear strongly at $\rho \geq 0.09$ nucleon/fm^3, where the fraction of nucleons that concentrate in clusters with mass number ($26 \leq A \leq 30$) reaches 19%. While it reaches 18% in clusters with mass number ($31 \leq A \leq 40$) and only 4% of nucleons were found in the heavier clusters ($41 \leq A \leq 50$).

5.2.5 CLUSTERED SYMMETRIC NUCLEAR MATTER AT T = 10 MeV

Clustered symmetric nuclear matter composition at T = 10 MeV is identified by Fig. 5.11 and Fig. 5.12. The fraction of nucleons in clusters would have soft change beyond 0.07 nucleon/fm^3 because of the formation of clusters with mass number ($A \geq 26$) when we included clusters up to A = 50 in the calculations. In fact, the fraction of heavier clusters ($A \geq 26$) does not exceed 7% up to 0.1 nucleon/fm^3. On the other hand, the dominant clusters at this temperature if we included the 89 clusters are clusters with mass number ($2 \leq A \leq 30$) and the remaining ones would have negligible contribution reaches just 2% of symmetric nuclear matter. In

particular, a large fraction of nucleons would bound in clusters with mass number $(A \leq 10)$ at density less than 0.063 nucleon/fm^3. Beyond this density clusters with mass number $(11 \leq A \leq 20)$ become the dominant.

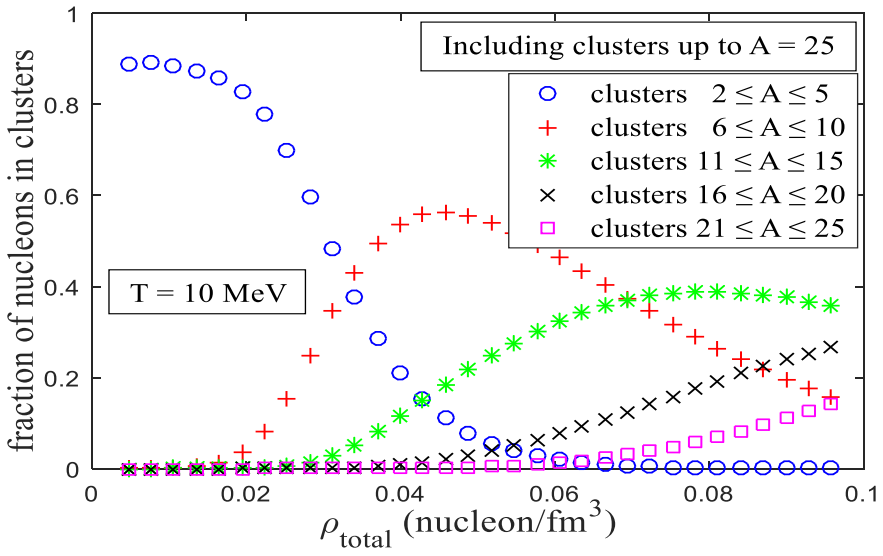

Fig. 5.11: Clustered symmetric nuclear matter composition at T = 10 MeV when the calculations included clusters up to A = 25 only.

Clusters with mass number $(2 \leq A \leq 5)$ are dominant till 0.031 nucleon/fm^3 even if heavier clusters up to A = 50 were included. These fractions reach 89% around 0.007 nucleon/fm^3 to 48% around 0.03 nucleon/fm^3. However, Clusters with mass number $(6 \leq A \leq 10)$ appear significantly in the density range 0.037 – 0.066 nucleon/fm^3 with their contribution reaching 56%. On the other hand, the fraction of nucleons in clusters with mass number $(11 \leq A \leq 25)$ has slightly changed when heavier clusters $(A \geq 26)$ were included in symmetric nuclear matter. Finally, we can note

that the fractions of nucleons which concentrated in clusters (A ≥ 26) do not exceed 5% along the whole density range up to 0.1 nucleon/fm^3.

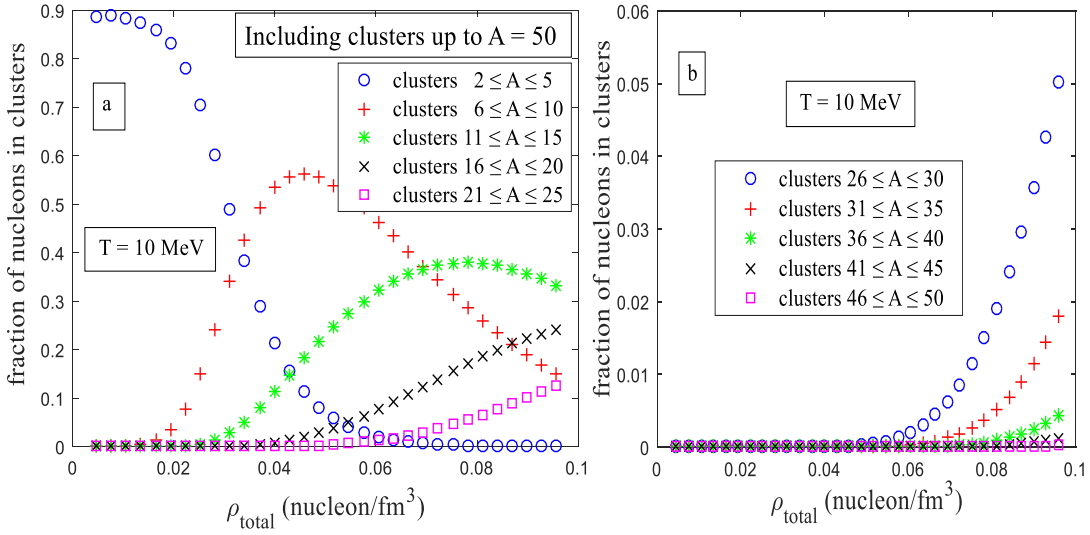

Fig. 5.12: Clustered symmetric nuclear matter composition at T = 10 MeV. The left part (a) represents the fraction of nucleons in clusters up to A = 25 when the clusters up to A = 50 were included in the calculations, whereas the right part (b) represents the fraction of nucleons in clusters 26 < A < 50.

5.2.6 CLUSTERED SYMMETRIC NUCLEAR MATTER AT T = 12 MeV

The fraction of nucleons in clusters as a function of density at T = 12 MeV is shown in Fig. 5.13 and Fig. 5.14. Clusters with mass number ($2 \leq A \leq 5$) are dominant till 0.047 nucleon/fm^3 where their contribution has a maximum of about 88% of the nuclear matter at ρ = 0.006 nucleon/fm^3 and falls down to about 45% at ρ = 0.047 nucleon/fm^3 when the next group of clusters starts to dominate. Whereas the nucleons would bound at 0.029 nucleon/fm^3 to form clusters with mass number ($6 \leq A \leq 10$),

and almost 55% of nucleons concentrate in these clusters around 0.064 nucleon/fm^3 before their gradual disappearance. On the other hand, clusters with mass number $(11 \leq A \leq 15)$ appeared beyond 0.04 nucleon/fm^3. Their fraction is increasing with density and reaches 36% as maximum at 0.1 nucleon/fm^3.

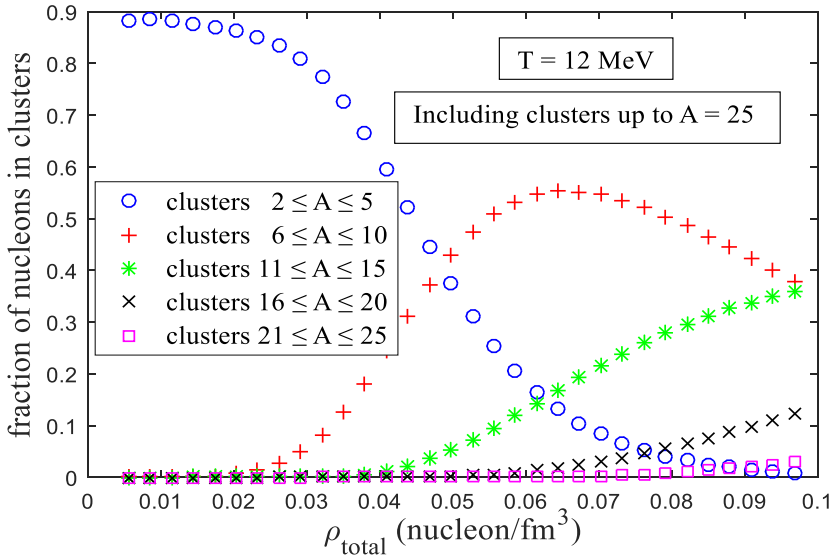

Fig. 5.13: Clustered symmetric nuclear matter composition at T = 12 MeV when the calculations included clusters up to A = 25 only.

Along the whole density range, the largest fraction of nucleons that have gathered to form clusters with mass number $(16 \leq A \leq 20)$ is 12%. While clusters with mass number $(21 \leq A \leq 25)$ contribution may be negligible as its fraction does not exceed 3%. Clusters with mass number $(A \geq 26)$ start to form beyond 0.06 nucleon/fm^3 but their fraction does not exceed 0.7%, so we can neglect their contributions in symmetric nuclear matter. Hence the composition of symmetric

nuclear matter at T = 12 MeV does not change even if we included more and more heavier clusters in the calculations.

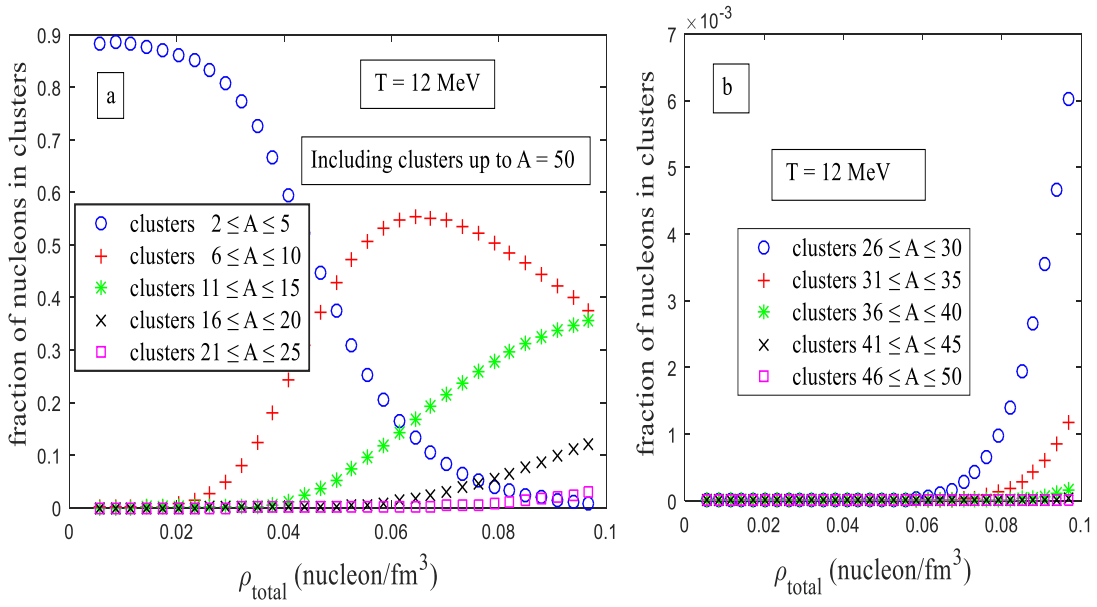

Fig. 5.14: Clustered symmetric nuclear matter composition at T = 12 MeV. The left part (a) represents the fraction of nucleons in clusters up to A = 25 when the clusters up to A = 50 were included in the calculations, whereas the right part (b) represents the fraction of nucleons in clusters 26 < A < 50.

In general, we can conclude that the cluster distribution depends on the symmetric nuclear matter temperature and density. At fixed temperature, the symmetric nuclear matter composition changes with increasing the total density such that correlations between a larger numbers of nucleons become significant. As a consequence, the fractions of clusters with smaller mass number decrease and the formation of heavier clusters increases as density increases.

On the other hand, the heavier clusters appear at higher density with increasing the symmetric nuclear matter temperature. However, the fractions of heavy clusters become negligible at high temperatures $T \geq 10$ MeV because of the lag in the lighter clusters dissolution.

Clusters with mass number up to 50 play a significant contribution in symmetric nuclear matter composition at $T \leq 6$ MeV while at T = 8 MeV only clusters up to A = 40 have a significant presence. At T =10 MeV only clusters with mass number up to 30 are present while at T = 12 MeV only clusters with mass number up to 15 have a substantial contribution in symmetric nuclear matter.

Finally, including heavier clusters makes the study more reliable where the nucleons are distributed among different groups of clusters not in the heaviest one only.

CHAPTER 6

RESULTS AND CONCLUSION

In this chapter, we will show and discuss the effect of including clusters with mass number up to A = 50 on the equation of state of clustered symmetric nuclear matter. In the previous chapters, the composition of clustered symmetric nuclear matter was determined, and here we will show the effect of including these clusters on the clustered symmetric nuclear matter critical point.

6.1 CLUSTERED SYMMETRIC NUCLEAR MATTER EQUATION OF STATE

The pressure of clustered symmetric nuclear matter contains contributions from all its contents including the free nucleons and the clusters.

$$P = P_{free\ nucleons} + P_{clusters} \tag{6.1}$$

where $P_{free\ nucleons}$ is the pressure due to the free nucleons which is given by Eq. 2.3 for an ideal Fermi gas of nucleons. Whereas, $P_{clusters}$ is the sum of all cluster pressures. Each cluster type contributes a pressure which is given by Eq. 2.3 for an ideal Fermi gas if the cluster is fermionic or by Eq. 2.6 for an ideal Bose gas if the cluster is bosonic.

As illustrated in chapter 5, we must include the clusters in low and intermediate density symmetric nuclear matter and we cannot ignore them. Fig. 6.1 shows the differences between the equation of state of low density symmetric nuclear matter in different treatments; ideal gas of nucleons, nucleonic gas with Skyrme interactions and clustered symmetric nuclear matter treated by using modified NSE model – with clusters up to A = 50.

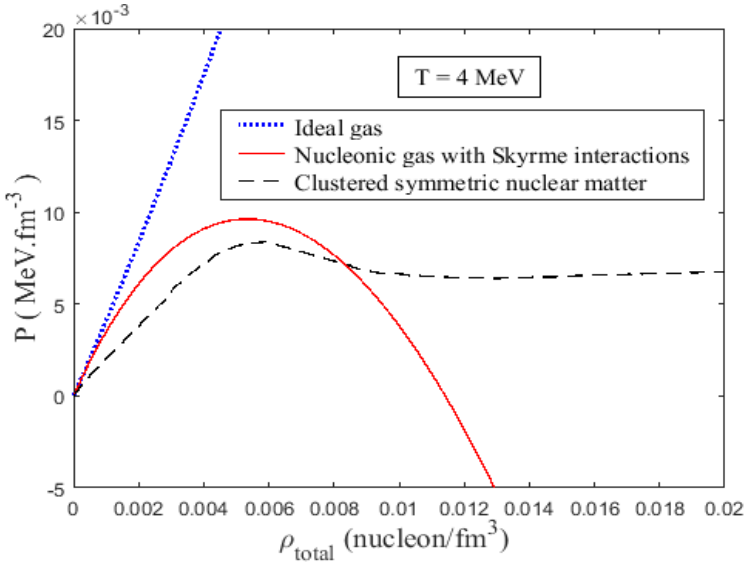

Fig. 6.1: Pressure isotherm at T = 4 MeV in different treatments; ideal gas of nucleons, nucleonic gas with Skyrme interactions and clustered symmetric nuclear matter with clusters up to A = 50.

The ideal fermi gas pressure increases monotonically with density. It is clear that the pressure of the ideal gas of nucleons and the pressure of Skyrme interaction nucleonic gas agree at extremely low densities as illustrated in Fig. 6.1. Whereas, clustered symmetric nuclear matter pressure isotherm has a different behaviour at low densities

due to the presence of clusters and their interaction with free nucleons. The interacting nucleonic gas pressure is larger than the pressure of clustered symmetric nuclear matter (due to the lower pressure of the bosonic clusters in the latter case), otherwise they have a similar behaviour increasing gradually with density up to a density of about 0.005 nucleon/fm^3. After that they both decrease with the pressure of the nucleonic gas dropping much faster.

We can note that clustered symmetric nuclear matter pressure isotherm after 0.005 nucleon/fm^3 decreases with increasing density up to 0.014 nucleon/fm^3 before it starts increasing again with density. Hence its behaviour is the same as nucleonic gas with Skyrme interaction pressure isotherm behaviour which is discussed in chapter 3. We will examine the effect of including clusters in symmetric nuclear matter on its equation of state by determining the critical point for clustered symmetric nuclear matter ($T_{critical}$, $\rho_{critical}$, $P_{critical}$) in the next section and comparing it with other studies.

6.2 COMPARISON BETWEEN THE RESULTS OF THE PRESENT WORK AND PREVIOUS STUDIES

Clustered symmetric nuclear matter pressure isotherms were drawn by using Eq. 6.1. We firstly include clusters with mass number up to A = 25 only before extending our calculation by including the remaining clusters with mass number up to A = 50.

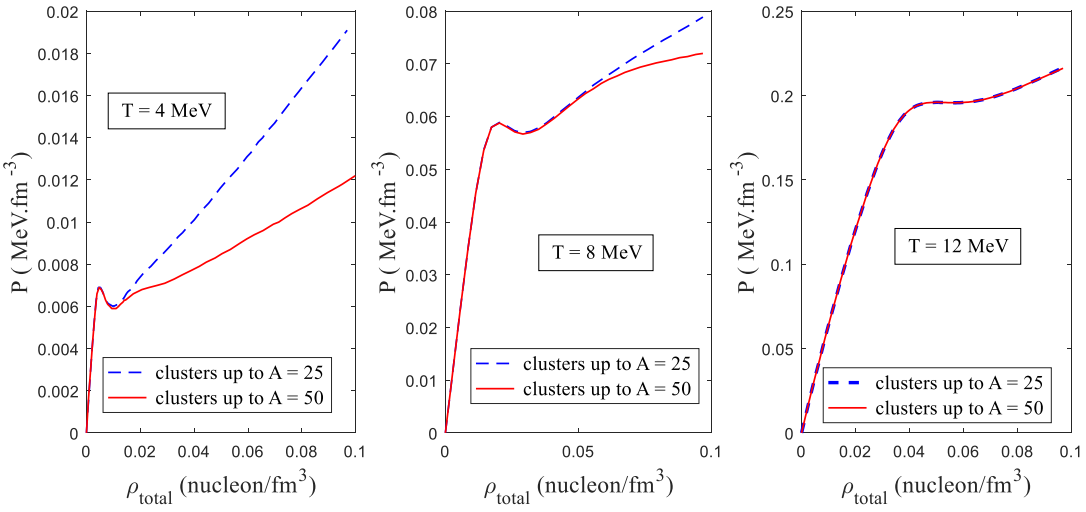

Fig. 6.2: Clustered symmetric nuclear matter pressure isotherms at three different temperatures; blue-dashed lines give pressure isotherms when only clusters up to A = 25 are included in the calculation, whereas the red-solid lines give pressure isotherms when clusters up to A = 50 are included in the calculation.

The pressure for clustered symmetric nuclear matter increases as temperature increases at specific density. However, it has lower values at high densities and fixed temperature when more and more clusters are included in the calculation as illustrated in Fig. 6.2 especially at low temperatures when the heavier clusters have significant contributions in symmetric nuclear matter. Regardless of the number of clusters included in the calculations the pressure isotherms have the same general behaviour similar to a van der Waals gas: the pressure initially increases with increasing density up to a certain value before it starts decreasing as the density increases and them finally increasing again as the density increases further).

Hence symmetric nuclear matter pressure isotherm does not change if we included clusters up to A = 50 at low densities but differs at higher densities due to the formation of heavier clusters, especially at low temperatures. For example, the change in pressure isotherm between the nuclear matter including clusters up to A = 25 and one with clusters up to A = 50 appears beyond 0.018 nucleon/fm^3 when heavier clusters start to form. At 0.1 nucleon/ fm^3 the pressure is reduced by about 0.008 MeV.fm^3 at T = 4 MeV and with same amount at T = 8 MeV where it is reduced from 0.078 – 0.07 MeV.fm^3 at 0.1 nucleon/fm^3. At T = 8 MeV the changes appear beyond 0.06 nucleon/fm^3 between the two cases. On the other hand, it is not affected at high temperatures ($T \geq 12$MeV) even at higher densities till 0.1 nucleon/fm^3 by including clusters up to A = 50. In general, the effect of adding heavier clusters to the calculations is important at lower temperatures.

The pressure isotherm at T = 12 MeV does not change by including the A > 25 clusters since its composition has a significant contribution from clusters with mass number up to A = 15 only. We also note that the critical point locates around T = 12 MeV. After studying the behaviour of pressure isotherms near T = 12 MeV, the critical temperature for clustered symmetric nuclear matter is 12.5 MeV where the pressure isotherm has one inflection point. Above this temperature clustered symmetric nuclear matter pressure isotherm increases as density increases and one fluid phase exists as shown in Fig. 6.3.

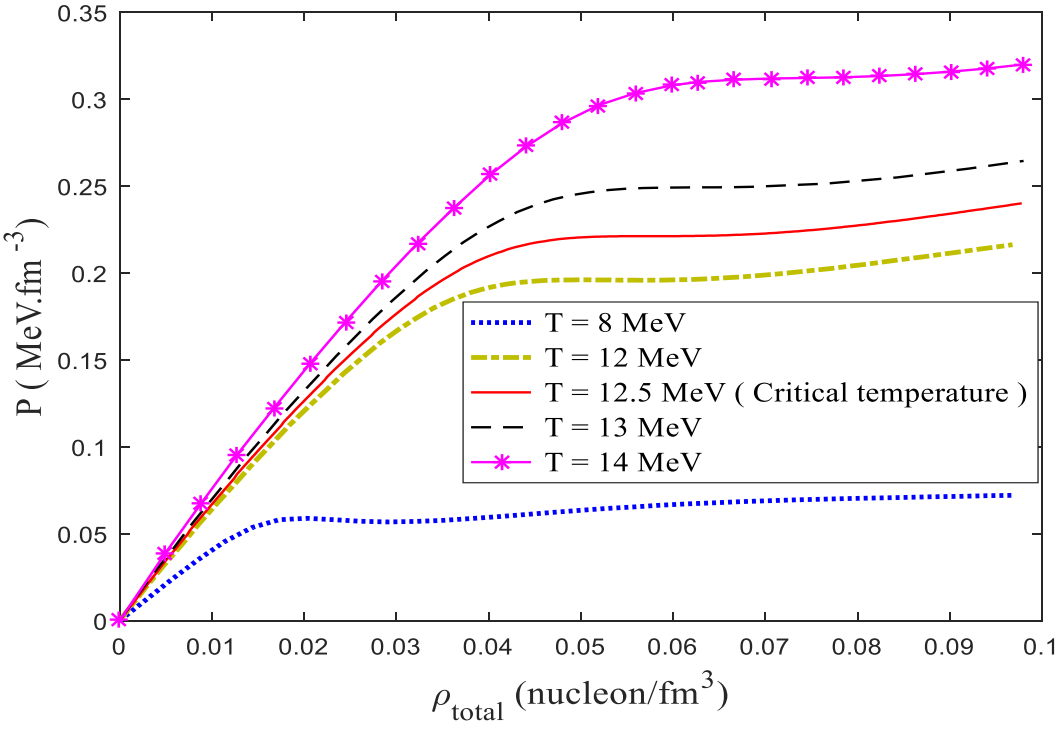

Fig. 6.3: Clustered symmetric nuclear matter pressure isotherm at different temperatures including the critical one.

Table 6.1 summarizes the parameters of the critical point obtained in the present work and in other studies. In most cases, including clusters tends to lower the critical temperature. The increase in $T_{critical}$ with the inclusion of clusters for the case of RMF is attributed by Typel et al to the overestimation of deuteron production (see Fig. 5.1). The main factor that makes our result change slightly from [19] is the differences between our Mott densities values and the ones that were used in [19].

Table 6.1: Critical point values obtained in the present work and in other studies.

	$T_{critical}$ (MeV)	$\rho_{critical}$ (nucleon/fm^3)	$P_{critical}$ (MeV.fm^{-3})
The present work (Including clusters with mass number up to A = 50)	12.5	0.0574	0.2211
The present work (Nucleons with Skyrme interactions)	17.32	0.058	0.2759
W. Awad [19] (Including clusters with mass number up to A = 25)	11.8	0.06	0.194
Typel et al [7] (RMF without clusters)	13.72	0.0452	0.1781
Typel et al [7] (RMF with light clusters [d, t, h and α])	15.12	0.1018	0.9029
Typel et al [7] (QS with light clusters [d, t, h and α])	12.1	-	-

6.3 CONCLUSION

Clusters with mass number up to A = 50 must be included in the equation of state of low and intermediate density symmetric nuclear matter especially at low temperatures where these clusters play a significant role in symmetric nuclear matter composition. The cluster distribution depends on both the temperature and density of symmetric nuclear matter. The light clusters up to A = 4 are dominant at very low densities whereas the heavier clusters appear at the higher densities where many-body correlations become significant. However, as temperature increases, the presence of the heavier clusters decreases gradually. At T = 12 MeV, only clusters up to A= 15 have a significant contribution.

In general, including clusters with mass number ($A > 4$) in low density symmetric nuclear matter reduces low density symmetric nuclear matter critical temperature by several MeVs in comparison with that obtained in [7, 14] where the clusters were not taken into account or just included light clusters with mass number up to A = 4.

In this work, we determined the composition of low and intermediate density symmetric nuclear matter by including light and medium clusters with mass number up to A = 50. The interactions between nucleons are taken into account only through cluster formation. To enhance this work, density-dependent effective masses of nucleons and clusters can be considered as medium modifications. Here, we dealt with Zero CM momentum clusters, future work can take into account CM momentum

of clusters which affects the binding energy of clusters and increase their Mott-densities.

This work can be used in astrophysical applications such as supernova explosions and to examine the early evolution of the universe by cosmologists. It is also important for the description of heavy ion collisions (HIC) in which light and medium nuclear clusters are formed.

BIBLIOGRAPHY

[1] G. Röpke, L. Münchow, and H. Schulz, "Particle clustering and Mott transitions in nuclear matter at finite temperature: (I). Method and general aspects," *Nuclear Physics A*, vol. 379, no. 3, pp. 536 - 552, 1982.

[2] G. Röpke, M. Schmidt, L. Münchow, and H. Schulz, "Particle clustering and Mott transition in nuclear matter at finite temperature (II): Self-consistent ladder Hartree-Fock approximation and model calculations for cluster abundances and the phase diagram," *Nuclear Physics A* , vol. 399, no. 2, pp. 587 - 602, 1983.

[3] H. R. Jaqaman, "Coulomb instability of hot nuclei," *Physical Review C*, vol. 39, no. 1, pp. 169 - 176, 1989.

[4] M. Beyer, S. Strauss, P. Schuck, and S.A. Sofianos, "Light clusters in nuclear matter of finite temperature," *European Physical Journal A*, vol. 22, pp. 261-269, 2004.

[5] H. Takemoto,M. Fukushima, S. Chiba, H. Horiuchi, Y. Akaishi, and A. Tohsaki, "Clustering phenomena in nuclear matter below the saturation density," *Physical Review C*, vol. 69, pp. 035802 – 035811, 2004.

[6] C. J. Horowitz, and A. Schwenk, "Cluster formation and the virial equation of state of low-density nuclear matter," *Nuclear Physics A*, vol. 776, pp. 55 - 79, 2006.

[7] S. Typel, G. Röpke, T. Klähn, D. Blaschke, and H.H. Wolter, "Composition and thermodynamics of nuclear matter with light clusters," *Physical Review C*, vol. 81, pp. 015803 - 015825, 2010.

[8] S. Typel, "Clusters in nuclear matter and the equation of state," *Journal of Physics: Conference Series*, vol. 420, pp. 012078 - 012092, 2013.

[9] Q. N. Usmani, N. Abdullah, K. Anwar, and Z. Sauli, "Nuclear matter properties, phenomenological theory of clustering at the nuclear surface, and symmetry energy," *Physical Review C* , vol. 84, pp. 064313 - 06431369, 2011.

[10] H. Togashi, K. Nakazato, Y. Takehara, S. Yamamuro, H. Suzuki, and M. Takano, "Nuclear equation of state for core-collapse supernova simulations with realistic nuclear forces," *Nuclear Physics A*, vol. 961, pp. 78 - 105, 2017.

[11] Ad. R. Raduta, and F. Gulminelli , "Statistical description of complex nuclear phases in supernovae and proto-neutron stars," *Physical Review C* , vol. 82, pp. 065801 - 065840, 2010.

[12] M. Hempel, and J.Schaffner-Bielich, "statistical model for a complete supernova equation of state," *Nuclear Physics A*, vol. 837, pp. 210 - 254, 2010.

[13] G. Röpke, "Light nuclei quasiparticle energy shift in hot and dense nuclear matter," *Physical Review C*, vol. 79, pp. 014002 - 014017, 2009.

[14] S. Levit, and P. Bonche, "Coulomb Instability in hot compound nuclei approaching liquid-gas transition," *Nuclear Physics A*, vol. 437, no. 2, pp. 426 - 442, 1985.

[15] H. R. Jaqaman, "Instability of hot nuclei," *Physical Review C*, vol. 40, no. 4, pp. 1677 - 1684, 1989.

[16] K. Sumiyoshi, and G. Röpke, "Appearance of Light Clusters in Post-bounce Evolution of Core-Collapse Supernovae," *Physical Review C*, vol. 77, 2008.

[17] S. Heckel, P. P. Schneider, and A. Sedrakian, "Light nuclei in supernova envelopes: a quasiparticle gas model," *Physical Review C*, vol. 80, pp. 015805 - 015812, 2009.

[18] S. Talahmeh, and H. R. Jaqaman, "light cluster formation in low density nuclear matter and the stability of hot nuclei," *Journal of Physics G: Nuclear and Particle Physics*, vol. 40, pp. 015103 - 015111, 2013.

[19] W. Awad, "The abundances of light and medium size clusters in low density nuclear matter," Birzeit university, Master thesis 2016.

[20] S. Kowalski, J. B. Natowitz, S. Shlomo, R. Wada, K. Hagel, J. Wang, T. Materna, Z. Chen, Y. G. Ma, L. Qin, A. S. Botvina, D. Fabris, M. Lunardon, S. Moretto, G. Nebbia, S. Pesente, V. Rizzi, G. Viesti, M. Cinausero, G. Prete, T. Keutgen, Y. El Masri, Z. Majka, "Experimental determination of the symmetry energy of a low density nuclear gas," *Physical Review C*, vol. 75, pp. 014601 - 014608, 2007.

[21] J. B. Natowitz, G. Röpke, S. Typel, D. Blaschke, A. Bonasera, K. Hagel, T. Klähn, S. Kowalski, L. Qin, S. Shlomo, R. Wada, and H. H. Wolter, "Symmetry energy of dilute warm nuclear matter," *Physical Review Letters*, vol. 104, pp. 202501 – 202505, 2010.

[22] K. Hagel, R. Wada, L. Qin, J. B. Natowitz, S. Shlomo, A. Bonasera, G. Röpke, S. Typel, Z. Chen, M. Huang, J. Wang, H. Zheng, S. Kowalski, C. Bottosso, M. Barbui, M. R. D. Rodrigues, K. Schmidt, D. Fabris, M. Lunardon, S. Moretto, G. Nebbia, S. Pesente, V. Rizzi, G. Viesti, M. Cinausero, G. Prete, T. Keutqen, Y. El Masri, Z. Majka, "Experimental determination of in-medium cluster binding energies and Mott points in nuclear matter," *Physical Review Letters*, vol. 108, pp. 062702 - 062706, 2012.

[23] R. K. Pathria, and P. D. Beale, *Statistical mechanics*, 3rd ed.: Elsevier Ltd., 2011.

[24] S. Wong, *Introductory Nuclear Physics*, 2nd ed.: Weinheim: Wiley-VCH Verlag Gmbh & Co. KGaA, 2004.

[25] H. Jaqaman, A. Z. Mekjian and L. Zamick, "Nuclear condensation," *Physical Review C*, vol. 27, no. 6, pp. 2782 -2791, 1983.

[26] T. H. R. Skyrme, "The effective nuclear potential," *Nuclear Physics*, vol. 9, no. 4, pp. 615 - 634, 1959.

[27] D.Vautherin, and D.M.Brink, "Hartree-Fock calculations with Skyrme's interactions. I. Spherical nuclei," *Physics Review C*, vol. 5, no. 3, pp. 626 - 647, 1972.

[28] H. R. Jaqaman, A. Z. Mekjian, and L. Zamick, "liquid-gas phase transitions in finite nuclear matter," *Physical Review C*, vol. 29, no. 6, pp. 2067 - 2074, 1984.

[29] G. Röpke, N.-U. Bastian, D. Blaschke, T. Klähn, S. Typel, and H.H. Wolter, "Cluster virial expansion for nuclear matter within a quasiparticle statistical approach," *Nuclear Physics A*, vol. 897, pp. 70 - 92, 2013.

[30] G. Röpke, "Medium effects and quantum condensates in low-density nuclear matter," *Acta Physica Polonica B*, vol. 3, no. 3, pp. 649 - 658, 2010.

[31] M. Ferreira, and C. Providência, "Nuclear matter EOS with light clusters within the mean-field approximation," in *Compact Stars in the QCD Phase Diagram III (CSQCD III) conference*, Brazil, 2012.

[32] A. Z. Mekjian, "Explosive nucleosynthesis, equilibrium thermodynamics, and relativistic heavy-ion collisions," *Physical Review C*, vol. 17, no. 3, pp. 1051 - 1070, 1978.

[33] M. Stein, A. Sedrakian, X-G. Huang, J.W. Clark, and G. Röpke, "Inhomogeneous condensates in dilute nuclear matter and BCS-BEC crossovers," *Journal of Physics: Conference Series*, vol. 496, 2014.

[34] K. Hagel, J. B. Natowitz, and G. Röpke, "The equation of state and symmetry energy of low density nuclear matter," *The European Physical Journal A*, vol. 50, pp. 39 - 54, 2014.

[35] A. Abdul-Rahman, M. Alstaty, and H. R. Jaqaman, "Centre of mass motion and the Mott transition in light nuclei," *Journal of Physics G: Nuclear and Particle Physics*, vol. 42, pp. 055111 - 055123, 2015.

[36] G. Röpke, "Paramettrization of light nuclei quasiparticle energy shifts and composition of warm and dense nuclear matter," *Nuclear Physics A*, vol. 867, pp. 66 - 88, 2011.

[37] G. Röpke, "Nuclear matter equation of state including two-, three-, and four-nucleon correlations," *Physical Review C* , vol. 92, 2015.

[38] G. Audi, A.H. Wapstra, C. Thibault, "The AME 2003 atomic mass evaluation - (II). Tables, graphs and references," *Nuclear Physics A*, vol. 729, pp. 337 - 676, 2003.

[39] S. S. Avancini, C. C. Barros Jr., D. P. Menezes, and C. Providência, "α particles and the pasta phase," *Physical Review C*, vol. 82, pp. 02508 - 02522, 2010.

[40] M. D. Voskresenskaya, and S. Typel, "Constraining mean-field models of the nuclear matter equation of state at low densities," *Nuclear Physics A* , vol. 887, pp. 42 - 76, 2012.

APPENDIX A

ENTROPY OF CLUSTERED SYMMETRIC NUCLEAR MATTER

Typel et al [7] found that the entropy per nucleon for symmetric nuclear matter with light clusters up to A = 4 decreases with increasing density as illustrated in Fig. A.1 except for a small region at low densities and low temperatures where entropy increases as the clusters dissolve into free protons and neutrons in the surrounding medium. This made Typel et al conclude that the formation of clusters reduces the entropy per nucleon as compared to nuclear matter without clusters that is, consisting only of free protons and neutrons. We will show that this does not contradict with the Second Law of Thermodynamics.

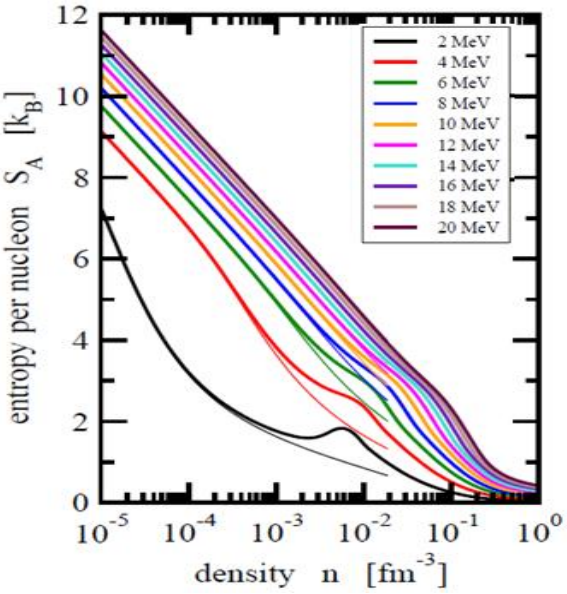

Fig. A.1: Symmetric nuclear matter entropy per nucleon S_A as a function of the total density n for different temperatures T. thick solid lines represent the result with including light clusters treated using RMF whereas the NSE calculation with light clusters but without considering their dissolution is represented by thin solid lines.

Typel et al are comparing between clustered symmetric nuclear matter and nuclear matter without clusters at constant temperature. What we want to emphasize is that it is not meaningful to compare at the same T, at least as far as the Second Law of thermodynamics is concerned.

The difference between the entropy of symmetric nuclear matter consisting of protons and neutrons only) and that of clustered symmetric nuclear matter appears strongly at low temperatures. We first note that the energy per nucleon for symmetric nuclear matter without clusters must remain the same after the formation of clusters due to energy conservation. As an example we evaluate the energy per nucleon for clustered symmetric nuclear matter at T = 6 MeV and $\rho = 0.001$ nucleon/fm^3 by using the following expression [23]:

$$\frac{E}{N} = \frac{3}{2}\, k_B\, T \left[f_{free\ nucleons} \frac{f_{5/2}(z_{free})}{f_{3/2}(z_{free})} + \frac{f_c}{A_c} \frac{f_{5/2}(z_c)}{f_{3/2}(z_c)} \right] - \frac{B_c f_c}{A_c} \qquad \text{A.1}$$

where $f_{free\ nucleons} = \frac{\rho_{\ free\ nucleons}}{\rho_{total}}$ is free nucleons fraction density, ρ_{total} is given by Eq. 4.3 with including light clusters up to A = 4 only, $f_c = \frac{\rho_c}{\rho_{total}}$ is the cluster fraction density, ρ_c is given by Eq. 4.4, A_c is the cluster mass number and B_c is the cluster binding energy which is given by Eq. 4.6. The functions $f_v(z)$ are defined by [23],

$$f_v(z) = z \pm \frac{z^2}{2^v} + \frac{z^3}{3^v} \pm \cdots \qquad \text{A.2}$$

where the upper sign is used for bosonic clusters and the lower sign is used for free nucleons and fermionic clusters, the fugacity $z = e^{(\mu/k_B T)}$ and μ is the chemical potential. The fugacity of cluster C is denoted by z_c and the fugacity of free nucleons is denoted by z_{free}. Finally, the chemical potentials of the clusters are given by Eq.4.2 while for the free nucleons the chemical potential is given by Eq.2.2 in the case of clustered nuclear matter.

From Eq. A.1 we find that the energy per nucleon $\frac{E}{N}$ (at T= 6 MeV and ρ = 0.001 nucleon/fm^3) = 4.2859 MeV for clustered symmetric nuclear matter. We mentioned above that the energy per nucleon for nuclear matter must be the same before forming clusters and after that. So the temperature for clustered symmetric nuclear matter will be higher than the corresponding temperature in the absence of clusters due to the absence of the cluster binding energy in the latter case. The energy per nucleon at low temperatures for symmetric nuclear matter with no clusters is given by the first term of Eq. A.1.

$$\frac{E}{N} = \frac{3}{2}\, k_B\, T \left[f_{free\ nucleons} \frac{f_{5/2}(z_{free})}{f_{3/2}(z_{free})} \right] \qquad \text{A.4}$$

On the other hand, nucleons in fact interact with each other by nuclear force. We used the Skyrme interaction which is mentioned in chapter 3 as a simple parameterization to describe the interactions between the nucleons. So the chemical potential for free

nucleons in the case of nuclear matter without clusters is given by Eq. 3.13, which was used in $f_v(z_{free})$.

So to keep the energy per nucleon conserved, the temperature of symmetric nuclear matter without clusters must be 2.784 MeV rather than 6 MeV. When the clusters form the excess energy released by the binding of the nucleons into the clusters raises the temperature, increasing it from 2.784 MeV to 6 MeV.

We estimated the entropy for symmetric nuclear matter with no clusters (free nucleons) by using the following expression [40]:

$$\frac{S}{N} = \frac{-1}{\rho} \frac{g}{(2\pi)^3} 4\pi \int k^2 \, dk \, [(1-f)\ln(1-f) + f \ln f \,] \qquad \text{A.5}$$

where $f = \{\exp(\beta\,[\varepsilon - \mu]) + 1\}^{-1}$, ε is given by Eq. 3.12 and μ is given by Eq. 3.13.

For clustered symmetric nuclear matter entropy we used Fig. A.1 which is taken from [7]. Table A.1 summarizes the differences in entropies per nucleon for both symmetric nuclear matter with clusters and without clusters (free nucleons).

Table A.1: Entropy per nucleon S/N for symmetric nuclear matter with no clusters and clustered symmetric nuclear matter at 0.001 nucleon/fm^3 and two different temperatures.

	Symmetric nuclear matter (free nucleons)	Clustered symmetric nuclear matter
	Entropy S/N [k_B]	Entropy S/N [k_B]
T = 2.784 MeV	4.0116	2.69
T = 6 MeV	5.1510	5.0

It is clear that the temperature of nuclear matter consisting of only nucleons without clusters increases from T = 2.784 MeV to T = 6 MeV when clusters are formed. Moreover, the entropy per nucleon increases from 4.0116 k_B to 5.0 k_B as required by the second law of thermodynamics. However, when we compare nuclear matter without clusters with nuclear matter containing clusters at the same temperature the one with clusters has lower entropy.